9-3-2013

Anchoring Energy of Dengue E Protein into Host Membranes and Quaternary Assembly Depend upon Lipid Composition

Briana Vernon

Briana C. Vernon

Candidate

Biomedical Engineering

Department

This thesis is approved, and it is acceptable in quality and form for publication:

Approved by the Thesis Committee:

Dr. Andrew P. Shreve, Chairperson

Dr. Michael S. Kent

Dr. Eva Y. Chi

ANCHORING ENERGY OF DENGUE E PROTEIN INTO HOST MEMBRANES AND QUATERNARY ASSEMBLY DEPEND UPON LIPID COMPOSITION

By

BRIANA C. VERNON

B.S. CHEMICAL ENGINEERING, UNIVERSITY OF NEW MEXICO, 2011

THESIS

Submitted in Partial Fulfillment of the
Requirements for the Degree of

Master of Science

Biomedical Engineering

The University of New Mexico
Albuquerque, New Mexico

July 2013

ACKNOWLEDGEMENTS

I would first like to thank Dr. Michael Kent for the opportunity to work in his lab for the past two years. It has been a blessing and privilege to do so, and I have learned much from his continuous instruction and insight. I am deeply grateful for the experience I have gained in working with Dr. Kent.

I would like to thank Dr. Andrew Shreve for his willingness to serve as my committee chair and for offering his time and expertise throughout the course of this thesis. I truly appreciate all of his advisement and guidance.

I would also like to thank Dr. Eva Chi for the lab experience I gained during my undergraduate studies that set a firm foundation for the work I have done during my graduate career. Her encouragement and advice have been very helpful.

In addition to my committee members, I would also like to acknowledge Sandia staff and post docs whose guidance and time in teaching me new skills I am grateful for: Nathan Bouxsein, Bryan Carson, Sadie La Bauve, Aaron Collins and Bryce Ricken.

Anchoring Energy of Dengue E Protein into Host Membranes and Quaternary Assembly Depend upon Lipid Composition

By

Briana C. Vernon

B.S. Chemical Engineering, University of New Mexico, 2011

M.S. Biomedical Engineering, University of New Mexico, 2013

ABSTRACT

Dengue virus is a devastating human pathogen responsible for millions of infections each year. No antiviral therapies for Dengue currently exist, making effective treatment of the virus challenging. Dengue is taken into the cell through endocytosis. Low-pH mediated structural rearrangements of the envelope protein E leads to the formation of fusogenic E trimers that facilitate membrane fusion with late endosomes. The fusion mechanism is not fully understood, but poses as a key target for inhibiting the viral infection pathway. An important aspect of fusion is the requirement of anionic lipids in the endosomal membrane. This study aims to characterize the biophysical reasons for this dependence by examining the role of anionic lipids in anchoring E to the membrane. E anchoring was investigated by sucrose gradient coflotation. We discuss the results of coflotation studies that were used to probe the unbinding of E trimers from liposomes of various compositions. We showed that E protein became unbound from liposomes over time when the membrane lacked anionic lipids, but remained bound to

liposomes containing anionic lipids. This demonstrates that anionic lipids facilitate greater anchoring of E to the membrane, which is essential for successful membrane fusion. Coflotation is commonly used to assess protein binding to membranes, but in this study coflotation is utilized as a novel methodology to probe weakly associated protein-membrane unbinding. To our knowledge, this is the first method of its kind. In addition, we also begin to investigate the role of anionic lipids in facilitating oligomerization of E trimers. We present preliminary results from sucrose gradient sedimentation and chemical crosslinking studies comparing trimer formation in the presence of liposomes with and without anionic lipids. Though further refinement of the trimer detection assays is necessary, sedimentation results suggest that trimerization occurred to a greater extent in the presence of anionic lipids. Taken together, our results reveal important functions of anionic lipids in facilitating membrane fusion useful for development of new therapeutic approaches.

TABLE OF CONTENTS

List of Figures

Figure 3.5 QCM-D binding curve with PC:PE bilayer and E protein. E was titrated into the chamber and monitored until little or no change in frequency and dissipation were detected. Concentrations of 0.1μM-5μM were examined. Maximum adsorption occurred around 5μm.

Figure 3.6 QCM-D frequency data expressed in terms of E protein coverage. Extent of E binding as a function of concentration reveals that adsorption occurred for both PC:PG and PC:PE at 0.1μM. The binding affinity is greater for PC:PG than for PC:PE.

Figure 3.7 Coflotation of 70:30 PC:PG and PC:PE liposomes with sE for 2.75hr at 54,000rpm. Membrane-bound protein is indicated by band intensity in the top three fractions. Much larger amounts of membrane-bound E were retained during centrifugation of PC:PG liposomes compared to PC:PE liposomes. For PC:PE, only trace amounts of protein were detected in Fractions 1 or 2. The presence of E in Fractions 4-10 indicates unbound protein is in the process of migrating to the bottom of the gradient.

Figure 3.8 Coflotation of 70:30 PC:PG and PC:PE liposomes with sE for 25hr at 54,000rpm. The difference in E anchoring to the two membranes is evident as protein remained bound to PC:PG membranes, but unbound from PC:PE membranes and sedimented to the bottom of the gradient.

Figure 3.9 Coflotation of 70:30 PC:PE liposomes with 6μM sE for 2.75hr at 54,000rpm. No bound protein was observed at higher concentration, demonstrating differences in E anchoring observed at 1μM are not a result of low protein coverage on PC:PE membranes compared to PC:PG membranes.

Figure 3.10 Coflotation of sE with 70:30 PC:PE liposomes at 27,000rpm for 2.75hr and 54,000rpm for 1hr. More protein was observed in the middle fractions at the lower spin time, while more complete sedimentation of protein resulted at lower rotor speed. In both cases, the vast majority of E still dissociated from the membrane.

dimer also present. Only trace amounts of trimer can be seen in Fraction 1, revealing far less trimerization in the membrane-bound state than anticipated.

Chapter 1

INTRODUCTION

1.1 Background and Global Threat of Dengue Virus

Dengue virus (DENV) is considered the most common arbovirus (i.e. arthropod-borne virus) and is currently endemic in more than 100 countries worldwide [1]. Disease transmission occurs by means of a specific mosquito vector (*Aedes aegypti*) prevalent in certain tropic and subtropic environments [2, 7]. As such, DENV is most prevalent in South America, Central America, select countries in Africa, and Southeast Asia, responsible for an estimated 50-100 million cases of infection each year worldwide [1-4, 6]. Of these, an estimated 500,000 cases result in hospitalizations and about 12,500 cases are fatal [6]. Dengue fever (DF) can produce symptoms that range from skin rash, headache, and muscle ache to joint pain and eye redness. More severe symptoms of internal bleeding and excessive fluid loss are associated with Dengue hemorrhagic fever (DHF) and Dengue shock syndrome (DSS). These ailments have the potential to become lethal and are more likely to develop upon secondary DENV infection [19]. Thus, in locations where DENV is rampant, the likelihood of repeat infection and life-threatening illness is greatly increased.

Currently, no antiviral therapies for DENV exist, making effective treatment of the virus challenging. Four different serotypes of the virus exist (DENV 1-4), which contributes to the difficulty in developing effective antiviral therapies for the disease and treating repeat infections. A patient that contracts DENV without having previous exposure will likely experience the symptoms associated with DF and will generally be

able to develop an immune response against that particular serotype. However, this immunity is only afforded against that serotype and not the other three available. Since four serotypes exist, the chance of contracting a heterotypic serotype of DENV upon secondary infection is high. Unfortunately, secondary infection leads to complications in a patient's antibody response, which make neutralizing the disease very challenging. It is believed that antibodies developed in response to primary infection actually enhance infection from a different serotype by causing large amounts of chemical mediators to be released from cells. This in turn causes membrane damage, and ultimately, endothelial cell leakage [2]. Heterotypic secondary infection thus promotes DHF and DSS symptoms by compromising cell membrane function.

1.2 **Structure and Lifecycle of DENV**

DENV is a spherical enveloped virus classified in the *Flaviviridae* family, which contains other significant flavivirus pathogens such as West Nile virus (WNV), tick-borne encephalitis virus (TBEV), and yellow fever virus (YFV). Common to flaviviruses is an envelope glycoprotein E that facilitates viral infection by promoting fusion of the viral and host cell membranes [1, 8]. The lipid membrane of the virion encapsulates the positive-sense RNA genome, which is released into the host cell upon fusion and replicated [2, 5]. The organization of a mature virus particle consists of three main structural proteins: the capsid protein (C), membrane protein (prM/M), and envelope protein (E) as shown in Figure 1.1a. The envelope protein is integral to successful infection of a host cell by promoting membrane fusion. Cryo-electron microscopy has

revealed that, in the native state, 90 E protein dimers pack in an icosahedral lattice, coating the outside of the virus particle, and lay tangential to the viral membrane in a head-to-tail fashion [5, 8, 28, 29]. A schematic of this protein organization is shown in Figure 1.1b.

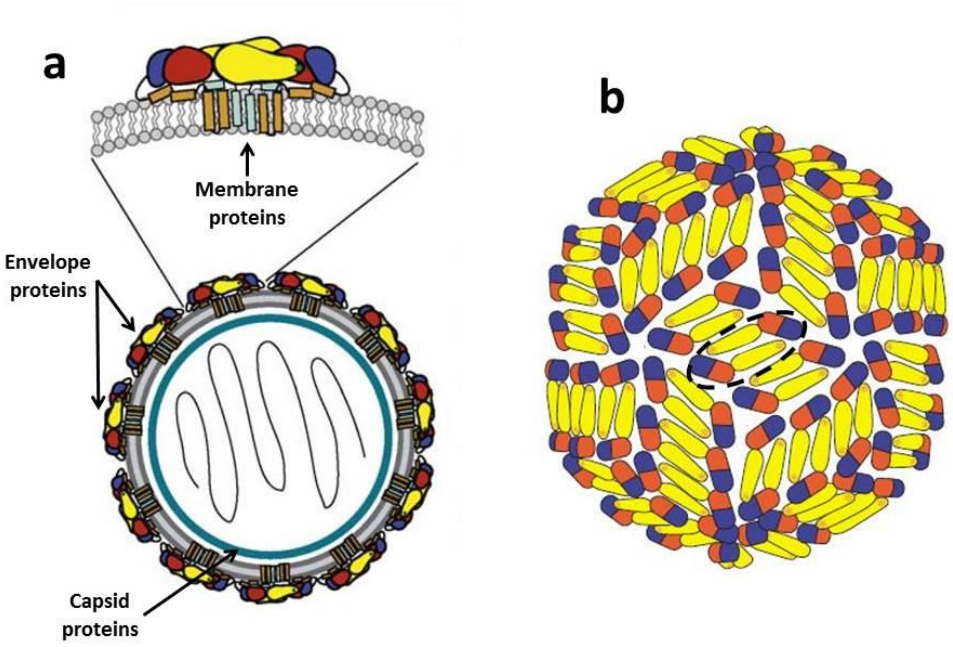

Figure 1.1: Organization of DENV structural proteins: (a) Structural proteins C, E, and M shown for a mature virion. Double grey lines represent the lipid bilayer surrounding the capsid, and the black line represents the viral RNA genome. Figure (a) adapted from [5]. (b) Arrangement of E protein dimers on mature virus surface. 90 dimers lay tangential to the lipid membrane and pack in an icosahedral lattice. A single dimer unit is highlighted in the center with a dashed black line. Figure (b) adapted from [8].

A complete understanding of the infection pathway would aid development of antiviral treatments for DENV. Figure 1.2 depicts the DENV lifecycle from internalization to replication and release. A description of the lifecycle events are as follows: Viral entry into the host cell is initiated when glycoprotein E of the mature virion binds to the surface of the cell via a cell-receptor-mediated interaction. Though E has been identified as the viral component responsible for initial cellular attachment, the exact cellular receptor(s) required for this interaction to take place have not been fully characterized. However, various reports identify a number of receptor molecules that enable DENV virus replication, each dependent upon such factors as the virus serotype and the cultured cell type. This suggests that DENV is able to bind multiple molecules for cell entry [1, 2, 9-11].

After the virus binds to the cell surface, it becomes internalized through endocytic uptake. Once the endosome forms, the internal environment gradually acidifies as the endosome matures, exposing the virus to the low pH environment. This change in pH triggers a drastic conformational rearrangement of E proteins on the surface of the virus, creating fusogenic trimers that facilitate membrane fusion between the viral and endosomal membranes [34, 35]. Membrane fusion releases the nucleocapsid of the virus into the intracellular environment, where the cell's machinery is utilized to replicate the RNA genome and assemble copies of the nucleocapsid. The virus progeny assemble by budding into the endoplasmic reticulum (ER) and are transported through the host secretory pathway [12]. At this point, the virions are considered immature, since E is associated with the prM (pre-membrane) protein complex. Before release at the cell surface via exocytosis, further processing of the prM complex takes place within the

Trans-Golgi network (TGN). Here, the pr peptide (used to prevent premature viral fusion during transit through the low pH environment of the TGN) is cleaved by a host-encoded furin protease [3, 20, 21]. The mature infectious virus progeny is then released into the extracellular environment to infect other cells.

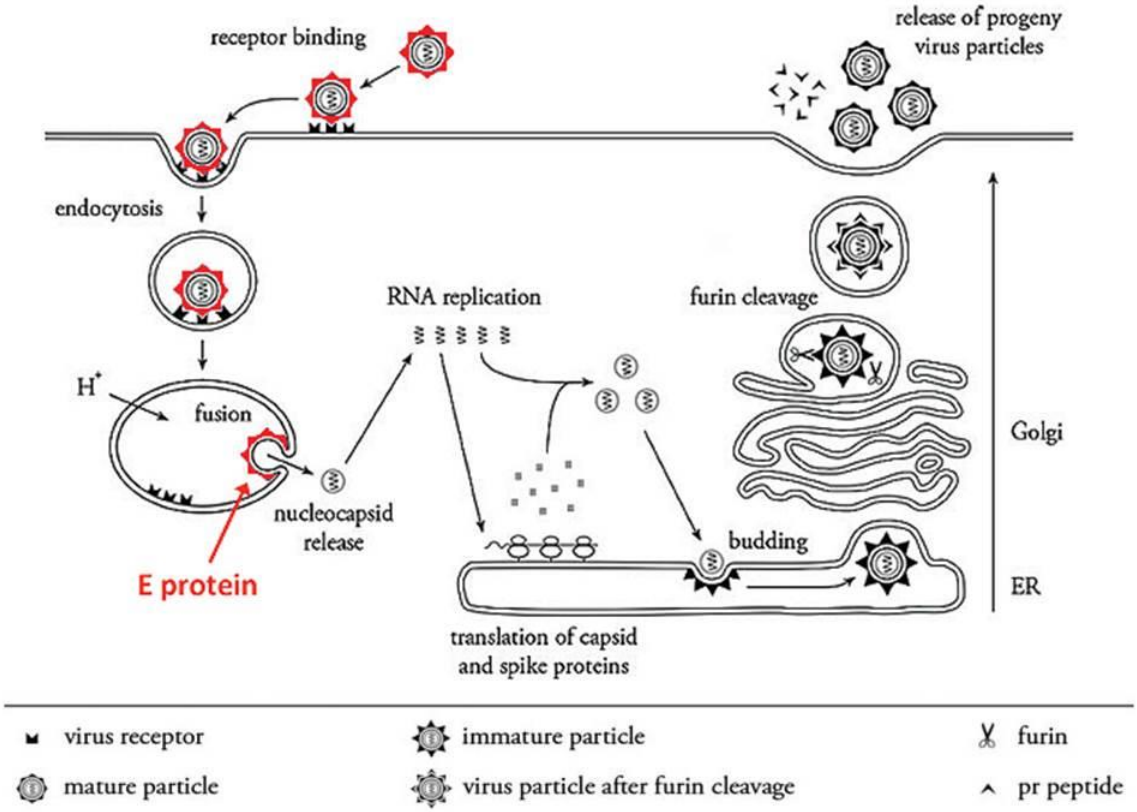

Figure 1.2: DENV lifecycle: Cell-receptor-mediated binding initiates virus internalization. Acidification in the late endosome triggers fusogenic E protein trimer formation enabling membrane fusion. RNA replication and viral budding in the ER are followed by furin cleavage in the TGN. Mature infectious virions are released to the extracellular environment via exocytosis. Figure adapted from [2].

1.2.1 Dengue E Fusion

Details regarding the membrane fusion mechanism within the DENV lifecycle are not fully understood, though its characterization has been the focus of many studies [3, 13-15]. The fusion process is of great interest as a therapeutic target, since it is a critical part of the infection pathway. The E protein crystal structure has been determined for both the pre- and postfusion states, which has provided important insight into the fusion mechanism; however, speculation remains concerning the protein conformations and rearrangements that take place from one state to the other.

1.2.1.1 Prefusion and Postfusion E Protein Crystal Structure

Throughout the virus lifecycle, DENV E exists in one of three conformational states: immature state (before furin cleavage of the pr peptide), mature state, and fusion-activated state [16]. In its mature state, E exists as a dimer that lays tangential to the viral surface at neutral pH, preventing exposure of the fusion loops of each monomer subunit. E is comprised of three distinct domains. These are identified in the linear sequence of the soluble E protein shown in Figure 1.3a for DENV 2. Domain I (DI) is shown in red, DII is shown in yellow, DIII is shown in blue, the fusion loop is shown in green, and the trans-membrane anchor is indicated by blue cross-hatch. When in a non-activated state, the fusion loop is buried beneath DI and DIII, protected from the environment [16]. A ribbon diagram of the atomic crystal structure of soluble E dimer is shown in Figure 1.3b.

The third conformational state exists upon low pH exposure. Acidification causes E dimers to dissociate, exposing the fusion loops of each monomer. These fusion loops

associate with the lipid membrane and collect to form trimers that have a membrane-insertable hydrophobic "bowl" at the tip; in this state E is considered to be fusion-activated [8]. A ribbon diagram of the atomic crystal structure of soluble E trimer is shown in Figure 1.3c.

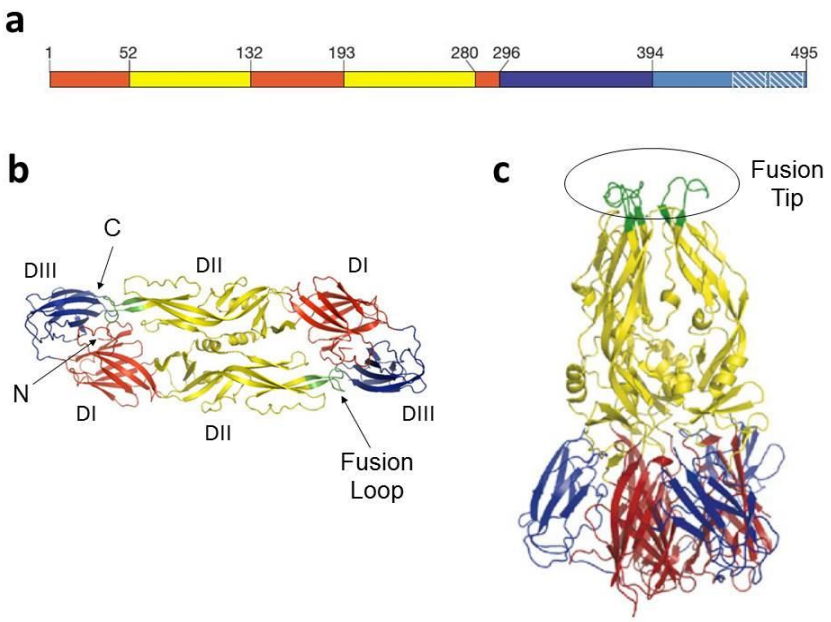

Figure 1.3: Soluble E protein structure: (a) 495 residue sequence of E monomer with DI in red, DII in yellow, DIII in blue, and trans-membrane region in blue cross-hatch. (b) Ribbon structure of prefusion E dimer. Domains I, II, and III are indicated, with DI located at the N terminus and the fusion loop located at the C terminus. Figures (a) and (b) adapted from [8]. (c) Ribbon structure of postfusion E trimer. Fusion loops from E monomers cluster to form a hydrophobic fusion tip. Figure (c) adapted from [16].

1.2.1.2 Hypothesized Fusion Mechanism

Understanding the prefusion and postfusion states of the E trimer has led to hypotheses regarding the intermediate states and conformational rearrangements that take place during fusion. Figure 1.4 depicts a hypothesized transition between the prefusion and the postfusion conformations leading to fusion. In Frame 1, the drop in pH causes E homodimers coating the viral surface to dissociate into monomers, which are shown anchored to the viral membrane (white) and able to insert the fusion loop into the target membrane (red) and form trimers. DIII begins to fold back against the DI/DII core, moving closer to the fusion loop. The stem region of the protein follows the rearrangement of DIII and begins to zip up along DII, as shown in Frame 2. Though it is not known how many trimers are needed to facilitate fusion, membrane alteration upon E insertion and the free energy associated with conformational changes of E are thought to be sufficient to make membrane fusion energetically favorable [18, 30-32]. Negative curvature develops around the inserted fusion loop, and the outer leaflets of the two membranes merge (hemifusion) as DIII folds back against DI and DII and the stem begins to zip up along DII (Frame 3). As association of the stem and DII is completed, full fusion of the membranes is achieved. Frame 4 depicts the final postfusion state of the E trimer, where the fusion loops and the transmembrane domains are now oriented on the same side of the protein [5, 14].

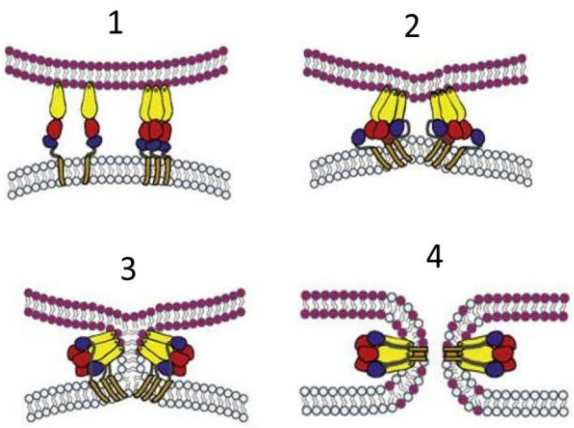

Figure 1.4: Proposed mechanism for membrane fusion: (1) Monomer fusion loop inserted into the target membrane (red). (2) Monomer clustering in the membrane forms fusogenic trimers and negative curvature begins to develop around the fusion loop. (3) DIII folds back towards the fusion loop and the stem region begins to pack against DII, resulting in hemifusion. (4) The stem associates with DII along the full length, achieving fusion and creation of a membrane pore; trimers are in the final postfusion state. Figure adapted from [5].

An important consideration that may help elucidate the fusion mechanism of DENV is to understand the function(s) that lipids in the target membrane have in the fusion process. Specifically, insight into how membrane composition and charge affect E protein binding, anchoring, and trimerization may provide key information. In that regard, studies have shown that DENV does not require cholesterol in the target membrane for efficient membrane fusion [22]. However, other studies have demonstrated that successful DENV fusion with plasma membranes, intracellular membranes, and model liposomes requires the presence of anionic lipids within the

membrane [13]. The biophysical explanation for this latter observation has not been identified. Therefore, further investigation of membrane charge dependence may provide answers to key questions regarding the fusion mechanism.

1.3 **Overall Aim and Accomplishments of This Work**

The goal of this work is to further elucidate the mechanism of membrane fusion that enables DENV infection and virus propagation. This knowledge will also be useful for understanding the fusion process of other important flavivirus pathogens that utilize similar fusion proteins and mechanisms for infection. The specific aim of this work is to examine the biophysical phenomena governing the membrane charge-dependence that enables DENV fusion. In this study, two hypotheses regarding the function of anionic lipids in the target membrane are examined: 1) Glycoprotein E anchoring into the host membrane is increased due to the presence of anionic lipids. Here, a centrifugation methodology has been developed to probe protein-membrane unbinding as a function of membrane composition. 2) Anionic lipids facilitate association of E into trimers and perhaps association of trimers into higher order structures. Though full understanding of how anionic lipids affect the oligomerization of E has not been achieved, an important foundation for further examination of this effect has been established as a result of this work. Finally, we note that membrane composition may also impact the fusion process through the extent of curvature induced upon E protein binding, but that topic is beyond the scope of this work.

The devastating effects of DENV serve as motivation to characterize the infection pathway of the virus with the aim to develop antiviral therapies that inhibit key steps of the infection pathway. No therapies currently exist to treat DENV, and further understanding of the viral fusion mechanism may reveal potential targets for inhibition. Knowledge of the function of anionic lipids in the fusion process will lead to important insights regarding the overall fusion mechanism, and may lead to the development of new therapeutic approaches.

Chapter 2

CHARACTERIZATION OF LIPOSOME MODEL MEMBRANES

2.1 Introduction

Liposomes are phospholipid vesicles composed of one or several concentric bilayers that encapsulate an aqueous core [25]. They are often used as a model to study protein interactions with the cell membrane, mimicking the lipid bilayer structure of cells. In addition, the membrane-like properties of liposomes have also been most notably explored for applications in targeted drug delivery systems, [26]. Liposomes are also useful to model other biological lipid membrane structures. Here, they are used to model the endosomal membrane for *in vitro* studies examining the differences in anchoring and oligomerization of E protein as a function of membranes composition.

Two of the most important characteristics that define liposomes are size distribution and lamellarity [39]. These qualities, in addition to chemical composition and surface properties, dictate liposome stability. Stability is a critical feature for many liposome applications and is generally divided into three categories: physical, chemical, and biological. The measurements described in this chapter examine the physical stability of liposomes before and after flotation through sucrose gradients as described in Chapter 3. Physical stability is reflected by both the uniformity in particle size distribution and the encapsulation efficiency of the vesicle (i.e. the ratio of lipid to entrapped volume) [41].

Extrusion through 100-200nm pores results in large unilamellar vesicles (LUVs) [24, 25], where 200nm pores are generally the largest diameter that still results in the formation of unilamellar vesicles. In terms of encapsulation efficiency, LUVs like those

used in Chapter 3 have a more constant lipid-to-volume ratio compared to multilamellar vesicles (MLVs). The varying number of bilayers in MLVs not only results in highly variable lipid content among the vesicles, but also alters the encapsulation volume.

In terms of size distribution, the liposomes used in Chapter 3 must be consistently monodisperse. Vesicles of this size are less likely to aggregate or fuse with one another in comparison to small unilamellar vesicles (SUVs), which are usually 50-100nm in size. Fusion and aggregation is more likely to occur with SUVs due to the higher stress curvature of the membrane [39]; thus, SUVs are less stable over time and become increasingly polydisperse. LUVs generally remain monodisperse due to lower stress curvature. The characteristics indicating the physical stability of liposomes are important to observe before and after flotation experiments to determine if the vesicles remain stable when subject to centrifugal forces in a high sucrose environment. The experiments described below demonstrate that unilamellar monodisperse vesicles used in Chapter 3 are indeed stable under the given centrifugation conditions and that they consistently float.

Verification of liposome stability is motivated by the need to ensure that liposomes used for coflotation experiments properly migrate through the gradient. This must be demonstrated in order to correctly interpret E protein coflotation data. The following experiments demonstrate that liposomes remain monodisperse and intact, and they migrate to the top of the gradient under the standard centrifugation conditions used for coflotation analysis (54,000rpm and 2.75hr). Centrifugation conditions of 27,000rpm at 2.75hr were also examined to confirm if liposomes still migrated appropriately at

slower rotor speed. Various time points were investigated to determine the minimum time necessary for flotation at these two speeds.

2.2 Experimental Section

2.2.1 Materials

Fluorescent liposomes were composed of a 70:30 molar ratio of 1-palmitoyl-2-oleoyl-sn-glycero-3-phosphocholine (POPC) and 1-palmitoyl-2-oleoyl-sn-glycero-3-phosphoethanolamine (POPE) or 70:30 molar ratio of POPC and 1-palmitoyl-2-oleoyl-sn-glycero-3-phosphatidylglycerol (POPG) with the addition of 3mol% fluorescent phospholipid 1,2-dioleoyl-*sn*-glycero-3-phosphoethanolamine-N-(5-dimethylamino-1-naphthalenesulfonyl) (ammonium salt) (Dansyl-PE) (Avanti Polar Lipids, Inc.). Each lipid component was dissolved in 9:1 solution of chloroform and methanol to form 2-3mg/ml stock solutions.

The lipid mixture was dried in a clean glass vial using a steady stream of nitrogen gas and then further dried for a minimum of 4hr up to overnight under vacuum to remove excess solvent. The lipid film was rehydrated for 10min in TAN buffer (20mM triethanolamine, 130mM NaCl, pH 8.0) and vortexed for 1min. Two cycles of hydration and vortex agitation were performed to release all lipids from the vial wall. Liposomes were then subject to 10 freeze/thaw cycles alternating between dry ice and warm water bath, followed by 21-pass extrusion (Avanti Mini-Extruder) through a 200nm polycarbonate membrane. Prepared liposomes were stored at 4˚C and used within two

weeks of preparation [3, 14, 17]. Dansyl-PE liposomes were used for both fluorescence and DLS measurements described below.

2.2.2 Methods

2.2.2.1 Fluorescence Measurements

E protein-membrane unbinding was probed by liposome coflotation assays, as described in further detail in Chapter 3. In order for coflotation to reveal meaningful information about protein-membrane unbinding, it must first be confirmed that the liposomes properly migrate through the sucrose environment and form a band at the top of the gradient under each of the centrifugation conditions examined.

Liposome flotation experiments were identical to protein-membrane coflotation experiments with two exceptions: 1) no E protein was included in the reaction mixture and 2) 3% Dansyl-PE was incorporated into the liposomes. Centrifugation was carried out under the same conditions as coflotation. Additionally, other time points were also examined to identify the minimum time and speed at which liposome flotation could still be achieved. 2µl samples of all 14 fractions were measured using a Nanodrop 3300 fluorospectrometer (Thermo Scientific). The relative fluorescence intensity of each fraction indicated the liposomes' location within the gradient after centrifugation.

2.2.2.2 Dynamic Light Scattering Measurements

DLS measurements were used to indirectly analyze the structural integrity of the liposomes after centrifugation. By examining the particle size distribution of the liposomes at the top of the gradient, one can determine if the liposomes remained intact during migration.

DLS analysis of liposomes in the top portion of the gradient requires a minimum sample volume of 1ml. To meet this requirement, gradients were scaled from the normal 700μl volume to a total volume of approximately 5ml using Beckman Ultra-Clear 13 x 51mm centrifuge tubes. The liposome sample was acidified, incubated for 30min at 28˚C, and then adjusted to 20% sucrose. To generate the gradient, 715μl of 40% sucrose was overlaid with 950μl of 20% sucrose, containing the liposome sample. 2.85ml of 15% sucrose was then deposited over the sample layer, and lastly, 480μl of 5% sucrose was added on top to complete the gradient. All sucrose solutions were made in MES buffer, pH 5.5. After centrifugation at 54,000rpm for 2.75hr, the top 1ml of the gradient was collected and dispensed into a disposable polystyrene cuvette for DLS measurement. The particle size distribution of the liposomes was analyzed using a Malvern zetasizer (Malvern Instruments Ltd., United Kingdom).

2.3 Results and Discussion

2.3.1 Fluorescence Measurements

Figure 2.1 displays fluorescence measurements for six different centrifugation conditions with both 70:30 PC:PG and PC:PE liposomes. Two spin rates of 54,000rpm and 27,000rpm were examined, and time points ranged from 15min to 2hr 45min. The

fluorescence intensity of each fraction is shown in comparison to the 100% maximum fluorescence value representing the case in which all starting material were to be collected in the top fraction of the gradient.

Compared to one another, PC:PE and PC:PG liposome compositions demonstrated similar migration patterns under the same centrifugation conditions. However, varying the centrifuge spin rate and time impacted flotation differently. At 54,000rpm and 2.75hr, liposomes consistently migrated to the top three fractions of the gradient, indicating that these conditions are sufficient to band liposomes at the top of the gradient. Decreasing time by a factor of five (0.5hr) at 54,000rpm still resulted in adequate flotation. However, as time was decreased further to 0.25hr, increased amounts of lipid appeared in later fractions.

The effect of time on flotation was observed for 27,000rpm as well. However, at this rotor speed, more time was required to achieve a similar degree of flotation compared to 54,000rpm. Equation 2.1 describes the relationship between rotor speed and force:

$$F = m_{buoy} r \omega^2 \qquad \text{Equation 2.1}$$

where F is force exerted on the liposomes, m_{buoy} is buoyant mass of the vesicles, r is distance from the axis of rotation, and ω is angular velocity. Considering force is proportional to angular velocity squared, at greater rotor speeds it follows that more force is applied to the gradient, causing liposomes to reach density equilibrium more quickly. Liposomes migrate according to their buoyant density and equilibrate to a region within

the gradient possessing similar density. The buoyant density of liposomes in the high sucrose environment causes the liposomes to band at the top of the gradient over time. Greater rotor speeds allow this equilibrium to be achieved in less time, as observed in the data.

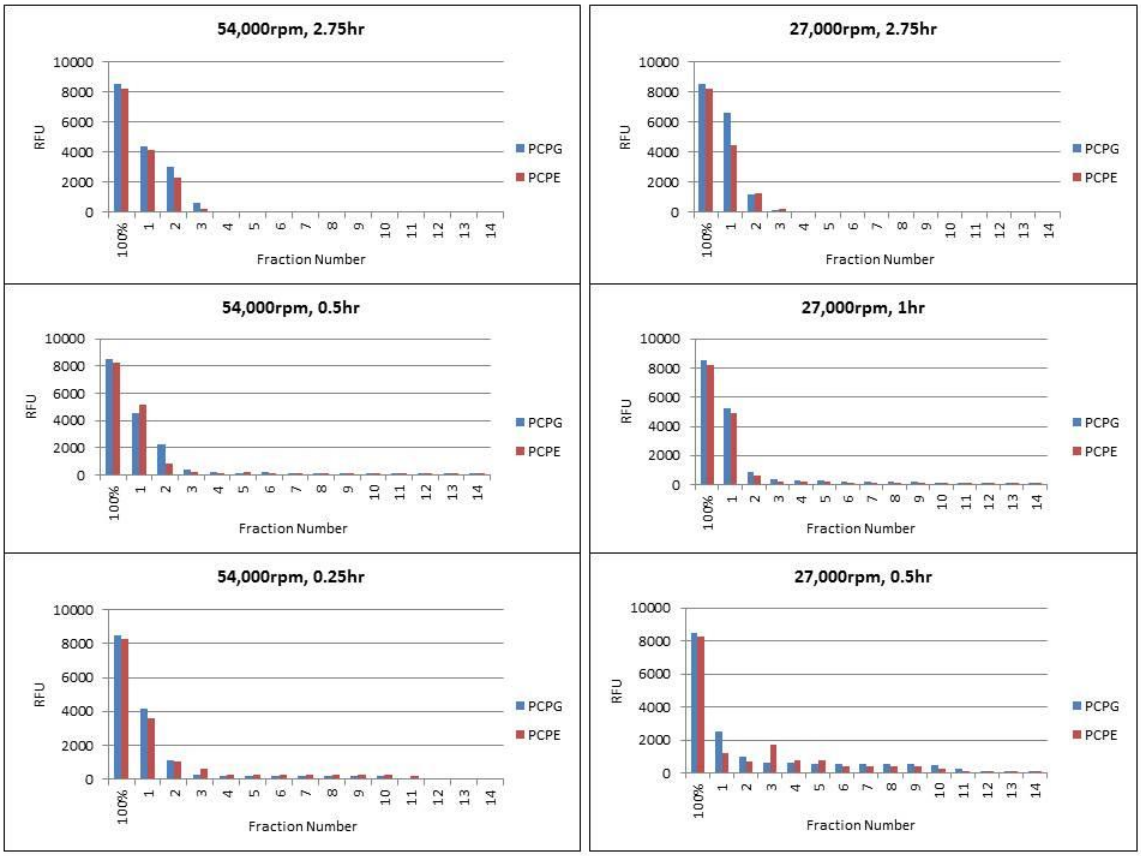

Figure 2.1: Liposome fluorescence measurements: Fluorescent liposomes demonstrate where vesicles migrate within the sucrose gradient for given centrifugation conditions. 70:30 PC:PE and PC:PG with 3% Dansyl-PE were examined at 54,000rpm and 27,000rpm, and time points ranged from 0.25hr to 2.75hr. Centrifugation at 54,000rpm and 27,000rpm had a minimum flotation time of ~0.5hr and ~1hr, respectively.

2.3.2 DLS Measurements

Figure 2.2 contains DLS data for both 70:30 PC:PG and PC:PE liposomes before and after centrifugation at 54,000rpm for 2.75hr. The data reveal that the starting liposomes and those contained in the top of the gradient after centrifugation are monodisperse. In addition, the liposomes also maintained a similar diameter before and after flotation. This result provides evidence that the liposomes remained intact as they migrated through the sucrose environment. If liposomes were to rupture due to shear forces or osmotic pressure imbalance, the resulting liposomes would likely become more polydisperse as the vesicles re-fused into various random sizes after breaking apart within the gradient.

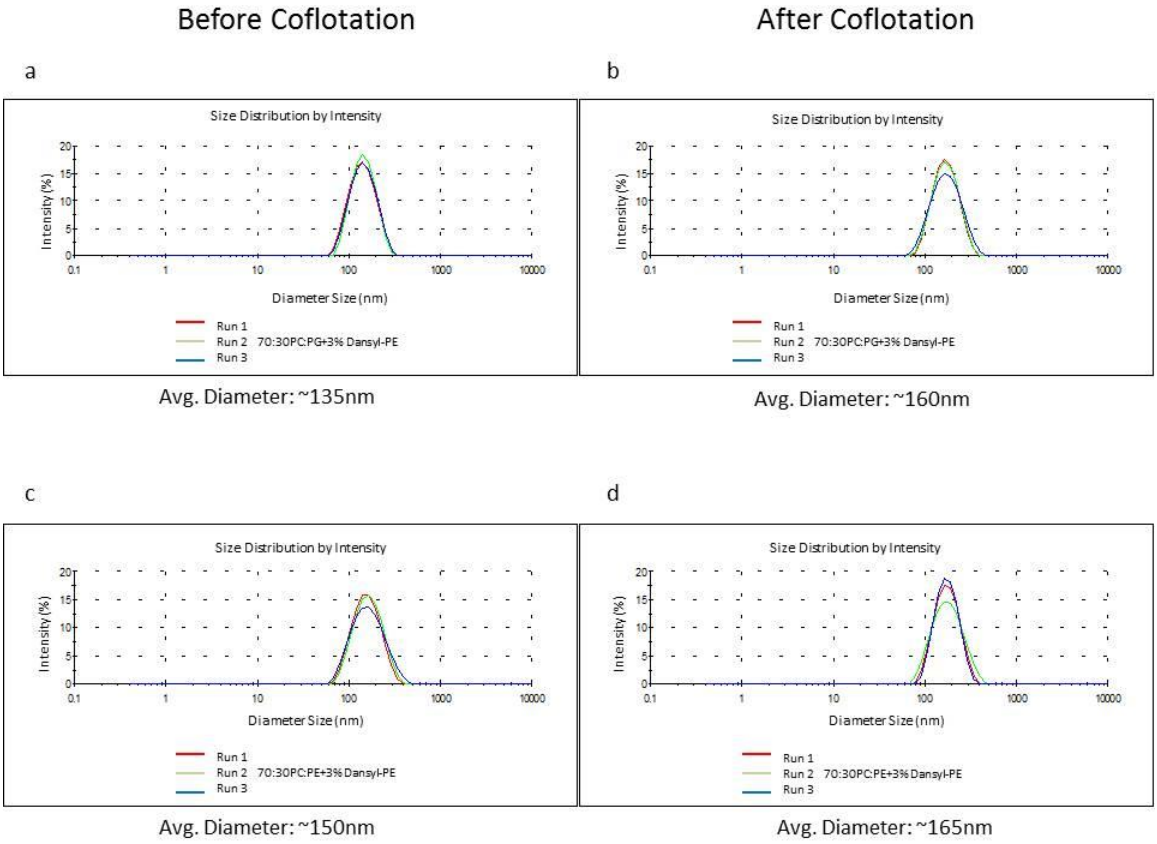

Figure 2.2: DLS measurements before and after liposome flotation: 70:30 PC:PG+3% Dansyl-PE liposome size distribution and average liposome diameter (a) before and (b) after flotation. 70:30 PC:PE+3% Dansyl-PE liposome size distribution and average liposome diameter (c) before and (d) after flotation. Similar monodisperse size distributions of liposomes before and after flotation for both compositions indicate the liposomes remain intact during flotation.

2.4 Chapter Summary

Both fluorescence and DLS measurements were used to demonstrate liposome stability and flotation efficiency under various centrifugation conditions. Fluorescence

measurements indicated that both 70:30 PC:PG and PC:PE liposomes migrate to the top three fractions of the gradient when spun at 54,000rpm for 2.75hr, demonstrating that these conditions used for coflotation experiments do indeed result in liposome flotation. Liposomes compared before and after centrifugation at 54,000rpm and 2.75hr remained monodisperse and had similar average diameters. Thus, DLS measurements demonstrate that liposomes remain intact as they migrate through the sucrose environment. In summary, these studies show that under the centrifugation conditions used for protein-liposome coflotation assays, liposomes properly float to the top of the gradient and do not rupture as they travel through the sucrose environment.

Chapter 3

E PROTEIN ANCHORING INTO TARGET MEMBRANE DEPENDANT UPON LIPID CHARGE

3.1 Introduction

Strong anchoring of E to the endosomal membrane is essential to the success of the fusion process. Anchoring to the host membrane must be sufficient to maintain the binding interaction despite large energies associated with substantial membrane bending that must occur during fusion. For instance, the energy barrier associated with membrane bending during hemifusion has been calculated in the range of 40 k_BT [56]. Prior work has established that DENV fusion requires the presence of anionic lipids in the target membrane [13]. We propose that anionic lipids enable fusion by facilitating greater anchoring of E to the membrane. Negatively-charged lipids may afford greater anchoring to the membrane through protein-membrane electrostatic interactions. It is also possible that the lower area per molecule of anionic lipids facilitates conformational changes in E after insertion of the fusion tip that leads to stronger anchoring. Though these specific mechanisms are beyond the scope of this work, Chapter 5 discusses how these ideas may be further examined for future studies.

Protein adsorption to a surface generally occurs in three steps: 1) protein transport to the surface from the bulk solution 2) interaction and reversible attachment of the protein to the surface 3) relaxation and rearrangement of the protein and/or the surface to achieve a lower energy state [45]. With this view of protein adsorption in mind, we postulate binding and anchoring interactions of E with the membrane as shown in Figure 3.1. After diffusing to the surface, adsorption of E to the membrane occurs (step 2),

likely through a combination of nonspecific electrostatic and dispersion interactions. This step is likely reversible at room temperature. However, insertion of the fusion loop into the membrane, possibly followed by conformational rearrangements of the protein and redistribution of lipids (step 3), leads to stronger anchoring of the protein into the membrane. This results in a higher energy barrier for unbinding (step 4) in which the off-rate is very slow at room temperature on experimental time scales. Since we propose that the free energy change characterizing unbinding of inserted E (step 4) may be substantially greater than that of initial binding (step 2), and since both steps are critical for membrane fusion to occur, experimental methods are needed to probe the unbinding of membrane-inserted E as well as initial membrane binding.

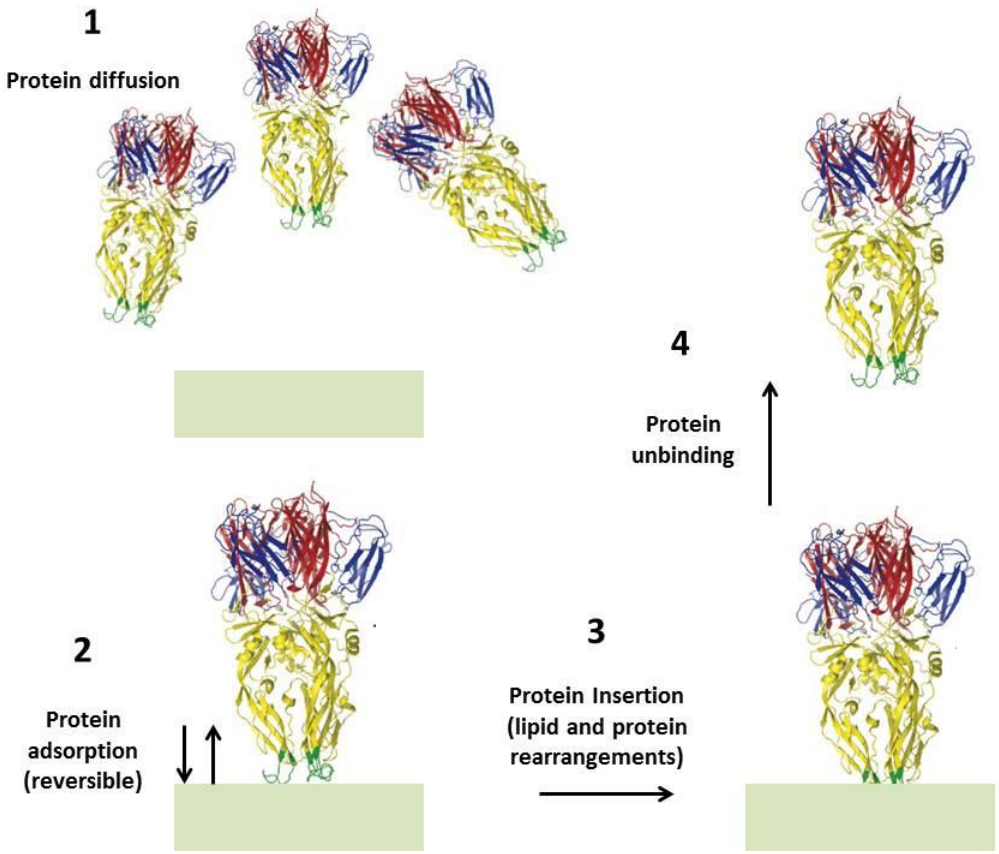

Figure 3.1: Schematic of E protein adsorption and insertion. Protein insertion is maintained by stronger anchoring to the membrane afforded by anionic lipids. E protein dissociation occurs more frequently due to weaker protein anchoring in membranes lacking anionic lipids.

Many methods have been developed to characterize protein adsorption [52]. However, few techniques have been developed to probe protein unbinding from surfaces, particularly for cases where the anchoring is strong enough that equilibration with free protein in solution is slow at room temperature. Atomic force microscopy (AFM) may be the only technique currently available to make such measurements [53]. However, measuring pull-out force of a protein by AFM is difficult. More importantly, AFM is limited in the range of forces it can measure. While AFM has been used to measure forces involved with pulling proteins out of membranes that are strongly associated, such as trans-membrane proteins [54, 57], in practice this technique is only able to measure pull-out forces down to ~10pN [55]. Studying the anchoring of proteins associated more weakly with membranes, only interacting with lipid headgroups or inserting into a single leaflet, may not be possible by this method. Based on electron microscopy images [8, 14] and the hydrophobic nature of the fusion loop, E trimer is thought to penetrate only a short distance into the hydrocarbon layer of the outer leaflet of the membrane [8]. This has been confirmed by recent neutron reflectometry data of the Kent group (unpublished)

that indicates E inserts into the lipid headgroups and only a few Å at most into the hydrocarbon tails of the outer leaflet. Therefore, in this work a new method was developed that is sensitive to anchoring energies of more weakly bound proteins that are still anchored strongly enough that they do not equilibrate with protein in solution on experimentally practical time scales. This new methodology is based on liposome coflotation *via* sucrose gradient centrifugation. The data below demonstrate that this method is able to probe membrane pull out for weakly associated membrane interactions, such as E trimer unbinding from liposomes. Coflotation is a common technique used to detect and separate membrane-bound from unbound proteins. This method has been used in many studies investigating the E protein binding interaction with membranes for flaviviruses and alphaviruses. In those studies, centrifugal force was used to separate bound from unbound protein, revealing how various protein mutations [3, 14, 17] or membrane compositions [22] affected binding.

Here, we have used similar coflotation methodology, not to investigate binding of E to the membrane, but to study E unbinding from the membrane and the variation in the rate of unbinding as a function of membrane composition. Understanding protein anchoring is an essential part of understanding the DENV fusion process. The following chapter demonstrates how coflotation methodology has been utilized to measure E protein unbinding, revealing key insights into the function of anionic lipids in facilitating stronger E protein anchoring.

3.2 Experimental Section

3.2.1 Materials

3.2.1.1 Liposome Preparation

Liposomes were composed of a 70:30 molar ratio POPC:POPE or 70:30 molar ratio of POPC:POPG. These liposome compositions were selected because fusion was observed for the 70:30 POPC:POPG liposomes in a VLP-liposome fusion assay, whereas no fusion was detected for 70:30 POPC:POPE liposomes in the same assay. Each lipid component was dissolved in 9:1 solution of chloroform and methanol to form 2-3mg/ml stock solutions. Liposomes were made according to the protocol in Chapter 2 Section 2.2.1 without the addition of fluorescent lipids. Briefly, the lipid mixture was dried, rehydrated for 10min in TAN buffer pH 8.0, and vortexed for 1min. Two cycles of hydration and vortex agitation were performed followed by 10 freeze/thaw cycles and 21-pass extrusion through a 200nm polycarbonate membrane. Prepared liposomes were stored at 4˚C and used within two weeks of preparation [3, 14, 17].

3.2.1.2 sE Expression, Purification, and Quantitation

E protein expression and purification protocols were followed according to prior published reports [3, 14, 17] and are concisely described here. Briefly, *Drosophila* S2 cells were stably transfected with plasmids containing either singly (sE'-ST) or doubly (sE'-STST) *Strep*-tagged Dengue virus serotype 2 (DENV 2). prME genes were grown in serum-free media (HyClone SFX-Insect, Thermo Inc.). Cells were seeded at $3X10^6$/ml in the presence of 750μM $CuSO_4$ and cultured with mechanical shaking for seven days at 26˚C. The supernatant was collected and filtered, then concentrated using 10kDa VivaFlow 200 cassette (Sartorius). The supernatant was adjusted to pH 8.0. *Strep*-

tagged DENV 2 E protein was purified using *Strep*-tactin Superflow Plus columns (QIAGEN) and quantified by UV spectrophotometry using a Nanodrop 2000c (Thermo Scientific).

3.2.2 Methods

3.2.2.1 Coflotation of sE and Liposomes

The methodology of liposome coflotation used to probe E protein anchoring into liposomes is as follows: unilamellar vesicles were combined with E protein and the reaction mixture was acidified. E protein interacts with the liposomes at low pH and binds to the lipid membranes. The reaction mixture was then deposited in a sucrose gradient, and upon centrifugation, membrane-bound and unbound E protein moved to different locations within the gradient according to the respective densities. Liposomes, and any associated protein migrated to the top of the gradient since the density of liposomes is lower than that of the sucrose layers. Unbound protein migrated to the bottom of the gradient since the density of protein is higher than that of the sucrose gradient.

Since other assays (described below) indicated that E bound to both liposome compositions, coflotation assays were performed to monitor the extent of protein that remained bound following centrifugation at various speeds and times. Solutions of 1μM and 6μM sE were combined with 1mM lipid and allowed to incubate for 30-60min at either pH 8.0 or pH 5.5.

Sucrose gradients were made in Beckman Ultra-Clear 5mm x 41mm centrifuge tubes in a total volume of 700µl. The volume for each layer was scaled down in relation to previous protocols that utilize larger volume tubes [3, 14]. Figure 3.2 shows a schematic of the gradient layers, along with the corresponding volumes and sample placement before centrifugation. Liposome-protein samples were adjusted to a 20% sucrose solution at a final volume of 133µl and applied to 100µl of a 40% sucrose cushion. The sample was overlaid with 400µl of a 15% sucrose solution followed by 67µl of a 5% sucrose solution. The pH of each sample was maintained within the gradient by using sucrose solutions made in TAN buffer, pH 8.0 or in MES buffer (50mM MES, 100mM NaCl), pH 5.5. Gradients were subject to centrifugation for times ranging from 2hr 45min to 25hr at speeds ranging from 27,000rpm to 54,000rpm at 4˚C using a Beckman SW55Ti rotor [3, 14, 17]. Figure 3.2 demonstrates the ideal protein separation achieved through coflotation. 50µl fractions were then collected from the gradient by hand using a glass syringe. A total of 14 fractions were collected.

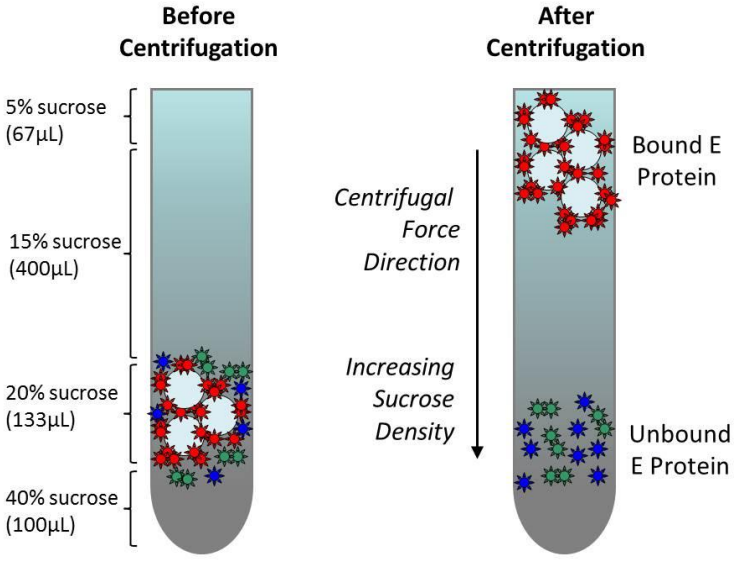

Figure 3.2: Schematic of coflotation gradient: Acidified protein-liposome reaction mixtures were adjusted to 20% sucrose and deposited within the gradient. Centrifugal force causes liposomes to form a band at the top of the gradient while unbound protein sediments to the bottom of the gradient. Bound protein migrates with the liposomes to the top of the gradient.

3.2.2.2 Low-pH Acidification and Incubation

sE protein alone or sE mixed with liposomes was acidified to pH 5.5 by the addition of a pre-calibrated volume of 0.3M MES, adjusted to pH 0.61. Samples were mixed by brief vortexing and then incubated at 28˚C for 30-60min. Samples were maintained at pH 5.5 and incorporated into sucrose gradients of the same pH.

3.2.2.3 Coflotation Fraction Analysis

Protein in each of the 14 fractions was analyzed by sodium dodecyl sulfate polyacrylamide gel electrophoresis (SDS-PAGE). 12μl samples were heated at 90°C for 5min and 10μl was loaded into NuPAGE 4-12% Bis-Tris polyacrylamide gels (Life Technologies). Gels were then stained using a Reversible Zinc Staining Kit (Thermo Scientific). Gels were placed in 25ml of zinc stain solution under gentle agitation for 10min. After removing the Stain solution, the gel was submerged in 25ml of zinc developer for ~1min. The gels were rinsed twice with water for ~1min after the

developer was removed. Gel images were collected immediately after staining protocol was complete.

3.2.2.4 QCM-D

sE binding curve studies were conducted using a quartz crystal microbalance with dissipation monitoring (QCM-D). Here, changes in the frequency (ΔF) and dissipation (ΔD) of an oscillating quartz crystal are used to measure the mass and rigidity of thin films that adsorb to the crystal surface. A Q-Sense D300 (Biolin Scientific) was used to acquire the data. Gold coated quartz crystal sensors were cleaned by boiling in 1:1:5 solution of NH_4OH, H_2O_2, and water for 25min. Sensors were rinsed with copious amounts of water and dried under N_2. Self-assembled monolayers of a lipid tethering compound were deposited by incubating the gold wafers in ethanolic solutions of 0.2mM *Z* 20-(*Z* octadec-9-enyloxy)-3,6,9,12,15,18,22-heptaoxatetracont-31-ene-1-thiol (HC18) and beta-mercaptoethanol (β-ME, Sigma Aldrich) in a 30:70 mol% ratio for ~18hr [49, 51] followed by extensive ethanol rinsing. Prepared sensors were then loaded into the sample chamber as shown below in Figure 3.3.

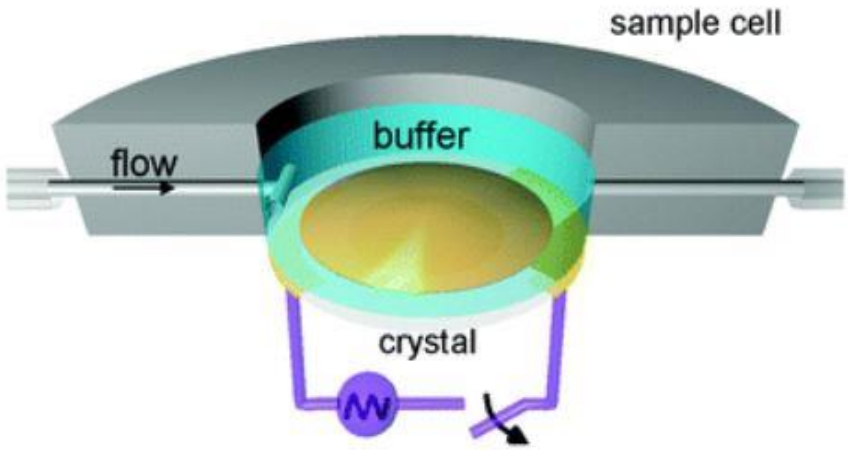

Figure 3.3: Schematic of QCM-D sample chamber: The prepared crystal was placed within the instrument, creating a sealed chamber to hold the liquid sample. A protein sample was flowed into the cell. The flow was stopped and the protein was allowed to adsorb to the lipid bilayer surface. Figure adapted from [50].

2ml of 2.5mg/ml PC:PE or PC:PG liposomes prepared in buffer (20mM MES, 500mM NaCl, pH 7.0) was flowed through the chamber. Flow was stopped and the liposomes were allowed to adsorb to the gold surface for 2-3hrs. The chamber was then exchanged with buffer containing lower salt concentration (50mM MES, 130mM NaCl, pH 7.0) causing the liposomes to rupture and fuse to the substrate and form a tethered lipid bilayer. After equilibrating for a few hours, E protein solutions ranging in concentration from 0.1μM-5μM were then added in succession. For each sample, sE was mixed into MES buffer pH 5.5 to the prescribed concentration in either 2ml (used for lower

concentration samples) or 1.3ml (used for 3μM and 5μM samples). 1.3ml is the minimum volume necessary to ensure a complete exchange of the cell volume.

3.3 Results

3.3.1 sE Binding Curves for PC:PE and PC:PG Membranes

QCM-D was used to indicate the level of E binding to PC:PE and PC:PG bilayers. Increasing concentrations of E protein were titrated into the sample chamber and allowed to equilibrate. The sensor response (ΔF and ΔD) versus time is plotted in Figure 3.4 for PC:PG and in Figure 3.5 for PC:PE. For the case of PC:PG shown in Figure 3.4, adsorption (indicated by drop in frequency) was detectable at 0.1μM, increased strongly from 1μM to 3μM, and began to level off at higher concentrations. The addition of protein at 5μM appears to bind in a non-specific manner as indicated by a gentle slope and slow adsorption rate compared to the previous concentrations. This weakly adsorbed protein was quickly removed from the surface by buffer exchange at the end of the experiment. Figure 3.5 shows the change in frequency and dissipation for a PC:PE bilayer over the same range of E concentrations. In this case adsorption was again clearly detectable at 0.1 μM, but the strong increase in concentration occurred at higher concentration (from 3μM to 5μM) than for PC:PG. Due to limited protein supply, concentrations higher than 5μM were not examined.

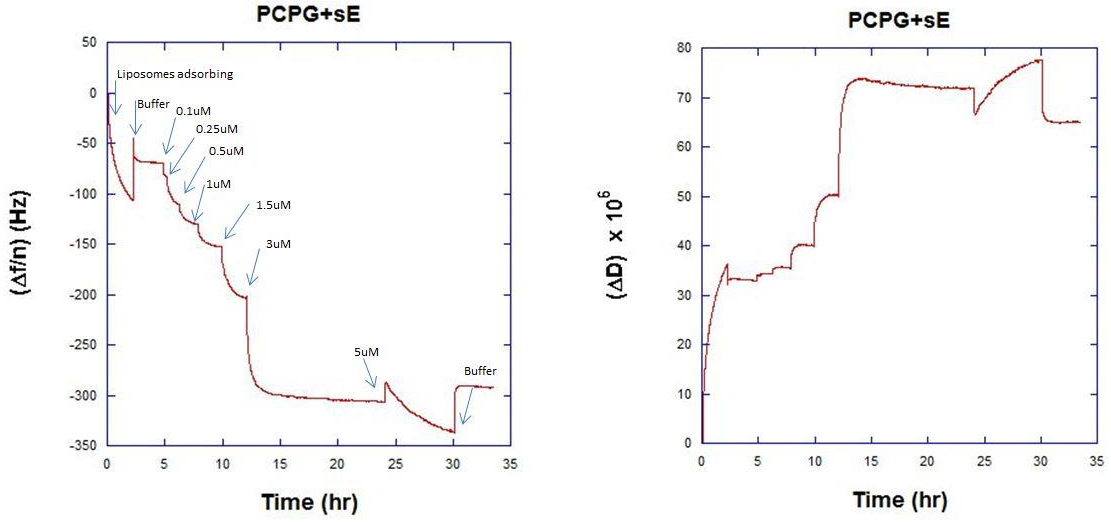

Figure 3.4: QCM-D binding curve for PC:PG bilayer and E protein. E was titrated into the chamber and monitored until little or no change in frequency and dissipation were detected. Concentrations of 0.1µM-5µM were examined. Maximum adsorption occurred around 3µm.

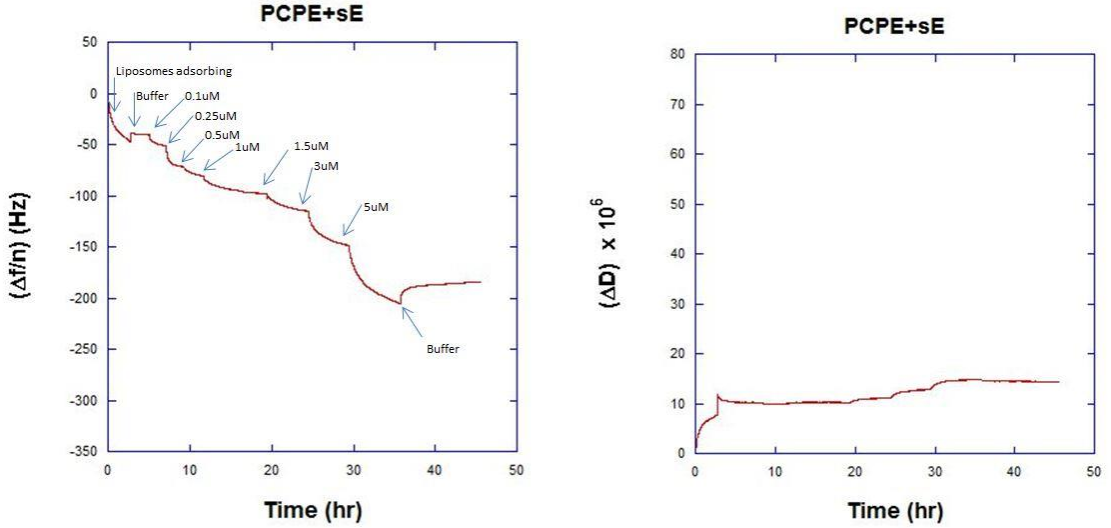

Figure 3.5: QCM-D binding curve for PC:PE bilayer and E protein. E was titrated into the chamber and monitored until little or no change in frequency and dissipation were detected. Concentrations of 0.1μM-5μM were examined. Maximum adsorption occurred around 5μm.

The measured change in frequency was converted to change in mass according to the Sauerbrey relation (Equation 3.1).

$$\Delta m = -\frac{C\Delta f}{n} \qquad \text{Equation 3.1}$$

where C is the mass sensitivity factor for gold coated quartz crystal (0.177mg/Hz/m^2) and n is the frequency overtone number. Figure 3.6 shows the change in mass plotted as a function of protein concentration. These results indicate that for both lipid compositions adsorption of E is detectable at 0.1 μM, and the binding affinity is higher for PC:PG than for PC:PE. Finally, we note that after flowing buffer through the cell at the end of each experiment, ΔF was nearly constant on the time scale of several hours for the case of PC:PG whereas ΔF increased steadily for the case of PC:PE. This indicates a gradual desorption of membrane-bound E from PC:PE but no detectable desorption of E from PC:PG.

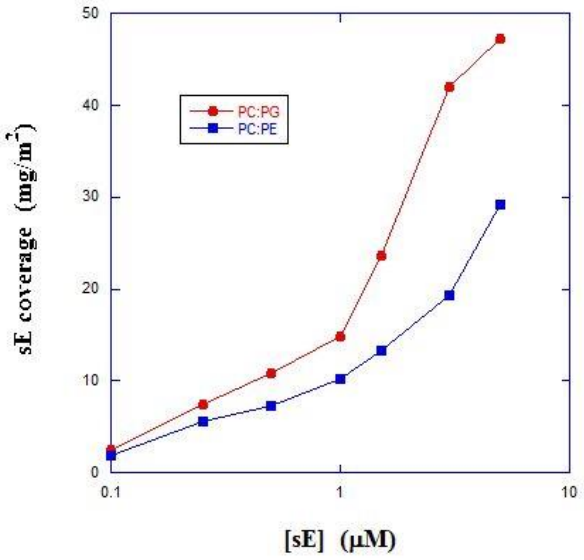

Figure 3.6: QCM-D frequency data expressed in terms of E protein coverage. Extent of E binding as a function of concentration reveals that adsorption occurred for both PC:PG and PC:PE at 0.1μM. The binding affinity is greater for PC:PG than for PC:PE.

3.3.2 Coflotation Separation of Unbound E Protein

Having determined from QCM that E adsorbs to both PC:PG and PC:PE membranes, coflotation assays were conducted with the same membrane compositions to probe the relative rates of protein unbinding. As shown in Chapter 2 through the use of fluorescent lipids, the top three fractions of the sucrose gradient contained the liposomes after centrifugation. Here, the top three fractions contain the membrane-bound protein as

well. Figure 3.7 reveals that upon centrifugation at 54,000rpm for 2.75hr substantial membrane-bound E is found with PC:PG liposomes, while hardly any membrane-bound protein is detectable with PC:PE liposomes. The measurements were conducted in triplicate to ensure reproducibility in the observed results and verify accuracy in fraction collection. Control measurements of E protein alone at both pH 5.5 and 8.0 shown in Figure 3.7 demonstrate that soluble E sediments in the bottom five fractions.

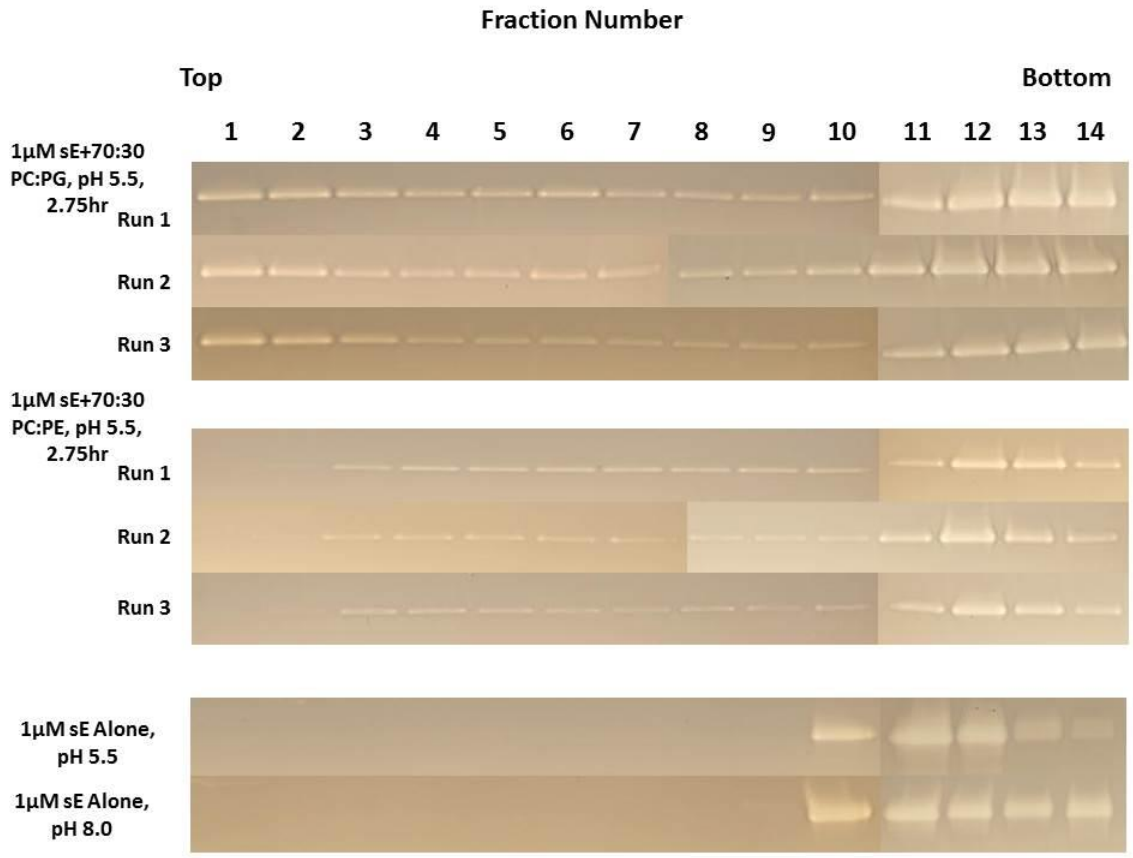

Figure 3.7: Coflotation of sE with 70:30 PC:PG and PC:PE liposomes at 54,000rpm for 2.75hr. Membrane-bound protein is indicated by band intensity in the top three fractions. Much larger amounts of membrane-bound E were retained during centrifugation of PC:PG liposomes compared to PC:PE liposomes. For PC:PE, only trace amounts of

protein were detected in Fractions 1 or 2. The presence of E in Fractions 4-10 indicates unbound protein is in the process of migrating to the bottom of the gradient.

In addition to bound E cofloating with liposomes in the top three fractions or unbound E sedimenting in the bottom five fractions, Figure 3.7 shows that some E appears consistently throughout the middle fractions of the gradient. This indicates that some protein must dissociate from the membrane during migration to the top of the gradient since it is not possible for E to migrate to higher fractions without being bound to a liposome.

The coflotation assay for PC:PG and PC:PE was also conducted at 54,000rpm over a time period of 25hrs. Comparing the results for PC:PE and PC:PG, Figure 3.8 again shows greater anchoring to membranes containing anionic lipids. Substantial amounts of E remained bound to PC:PG liposomes, and very little protein was observed in the middle of the column as the centrifugation time was long enough for protein that unbound from the membrane to sediment to the bottom of the gradient. For PC:PE membranes, nearly all the protein sedimented to the bottom of the gradient.

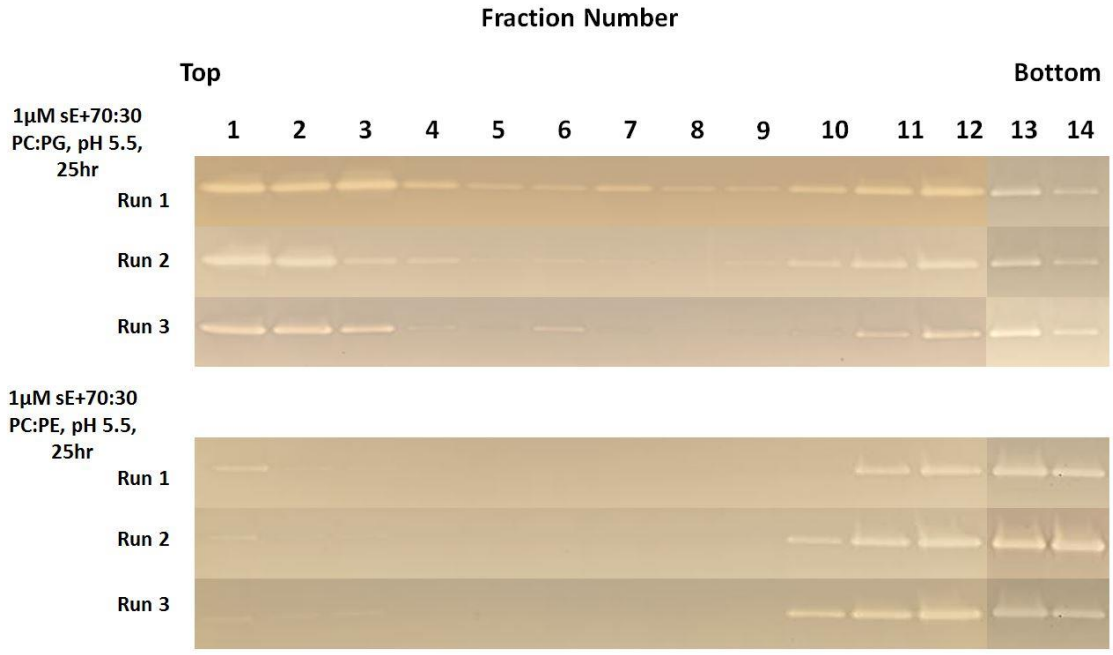

Figure 3.8: Coflotation of sE with 70:30 PC:PG and PC:PE liposomes at 54,000rpm for 25hr. The difference in E anchoring to the two membranes is evident as protein remained bound to PC:PG membranes, but unbound from PC:PE membranes and sedimented to the bottom of the gradient.

The coflotation assay was also performed for PC:PE membranes incubated with E at 6µM. The QCM adsorption data in Figure 3.6 indicates that the amount of E adsorbed to PC:PE membranes at 6µM is substantially greater than the amount adsorbed to PC:PG membranes at 1µM. Despite the greater amount of protein adsorbed following incubation, Figure 3.9 demonstrates that after centrifugation for 25hrs little or no E remained bound to the membrane. This shows that upon centrifugation E unbinds from

PC:PE membranes at a far greater rate than from PC:PG membranes, even when E is originally present on the membrane at a much higher coverage. The anchoring energy of E in PC:PE membranes is therefore far weaker than that for E in PC:PG membranes.

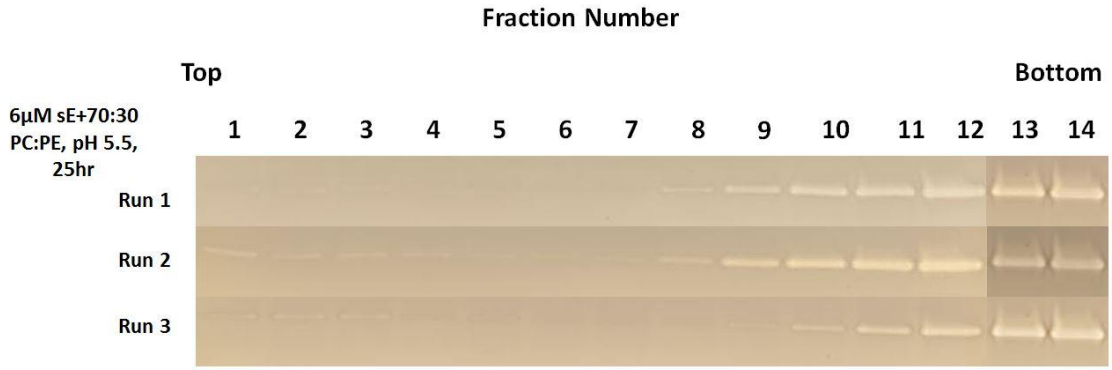

Figure 3.9: Coflotation of 70:30 PC:PE liposomes with 6μM sE for 2.75hr at 54,000rpm. No bound protein was observed at higher concentration, demonstrating differences in E anchoring observed at 1μM are not a result of low protein coverage on PC:PE membranes compared to PC:PG membranes.

While the results described above demonstrate a substantial difference in anchoring energy for E in PC:PG versus PC:PE membranes, further assays were performed to better understand this new methodology by further examining the relationships between anchoring energy, protein distribution throughout the column, and centrifugation parameters. Coflotation assays were performed for PC:PE membranes

using slower rotor speeds and reduced times. As shown in Figure 3.10, spinning the samples at 27,000rpm for 2.75hr resulted in E protein sedimenting at the bottom of the gradient. On the other hand, a coflotation assay for PC:PE membranes was also performed in which the spinning time was reduced to 1hr while the rotor speed was maintained at 54,000rpm. In that case Figure 3.10 shows greater band intensity in the middle fractions compared to the PC:PE data for 2.75hr in Figure 3.7.

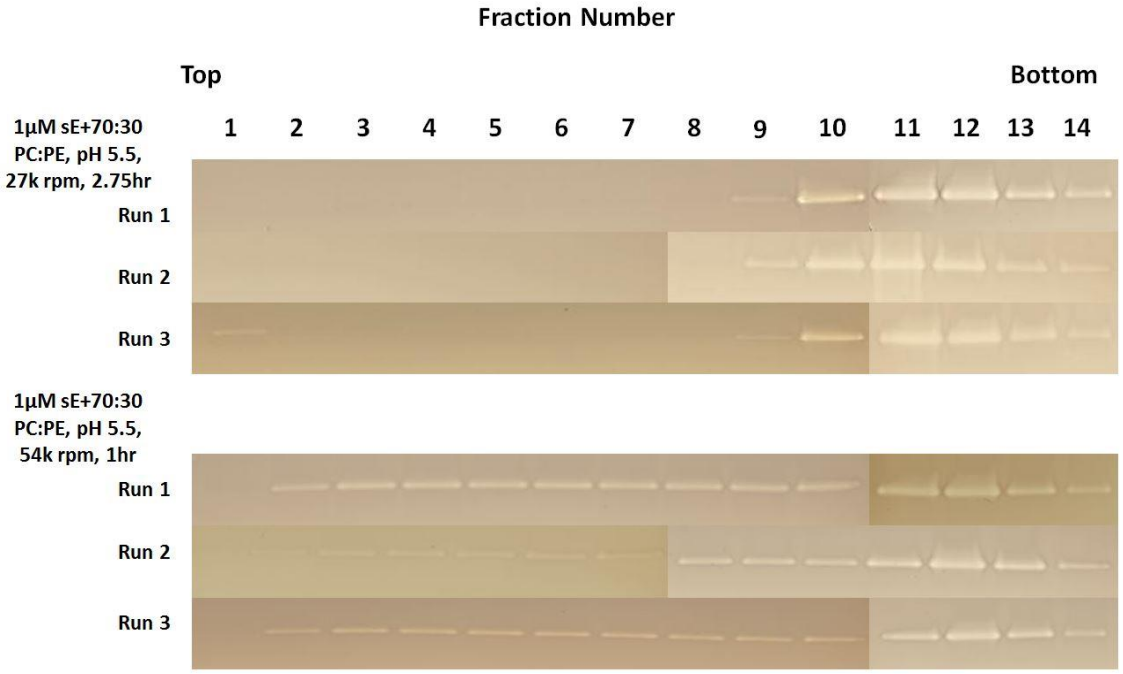

Figure 3.10: Coflotation of sE with 70:30 PC:PE liposomes at 27,000rpm for 2.75hr and 54,000rpm for 1hr. More protein was observed in the middle fractions at the lower spin time, while more complete sedimentation of protein resulted at lower rotor speed. In both cases, the vast majority of E still dissociated from the membrane.

In a further study, the amount of PG lipid in the membrane was reduced to 10mol% to examine the relationship between the amount of anionic lipid and the rate of protein unbinding under centrifugation. The coflotation assay was performed with 90:10 PC:PG liposomes. The results were compared to those for 70:30 PC:PG under the same centrifugation conditions of 54,000rpm and 2.75hr in Figure 3.7. Figure 3.11 shows that a small amount of binding still occurred at 10% PG, but binding clearly decreased with decreasing percentage of PG in the membrane.

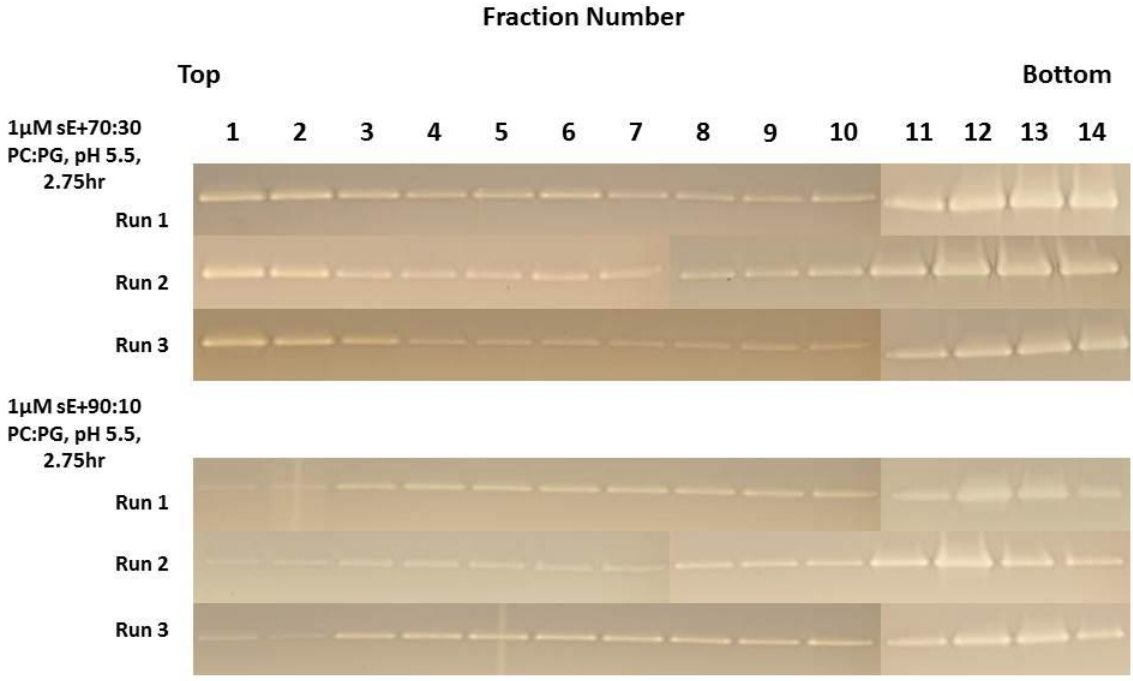

Figure 3.11: Coflotation of sE with 70:30 PC:PG and 90:10 PC:PG liposomes at 54,000rpm for 2.75hr. A small amount of binding occurred with 10mol% PG, while

30mol% PG facilitated a greater extent of binding. This confirms anchoring increases as a function of anionic lipid content.

3.4 Discussion

The coflotation results presented in the previous section clearly reveal a slower rate of E protein unbinding from membranes containing anionic lipids than from neutral membranes. However, to fully understand the relationship between protein distribution throughout the gradient and anchoring energy, we must determine the mechanism(s) by which centrifugation accelerates the rate of protein unbinding from lipid membranes. We begin by determining the impact of centrifugal and shear forces on the energy barrier for unbinding. It has been shown that relatively weak forces applied over a long time period can cause unbinding of molecules that associate through weak non-covalent interactions to occur at room temperature by slightly reducing the energy barrier [57].

Rotor speed and spin duration dictate the applied force throughout the gradient during centrifugation. Calculating the magnitude of this force and how it varies with rotor speed will elucidate if the centrifugal force can substantially alter the energy barrier for unbinding. From molecular dynamics simulations, the buoyant mass of an E trimer was determined to be 26.25kg/mol [44]. Considering a rotor speed of 54,000rpm, and assuming a liposome-bound trimer is positioned at the top of the gradient, the force on the bound E trimer according to Equation 2.1 is on the order of 10^{-5}pN. This is very weak compared to the force necessary to unfold globular proteins at typical experimental

rates, which is in the range of ~20pN [43]. In Figure 3.12, the energy landscape E(x) of a bound trimer molecule has been modeled as a function of distance from a liposome surface [44]. E(x) has also been modeled with the addition of the centrifugal force applied at 54,000rpm and 72,000rpm. It can be seen that the additional force from centrifugation does not significantly lower the energy barrier at those rotor speeds.

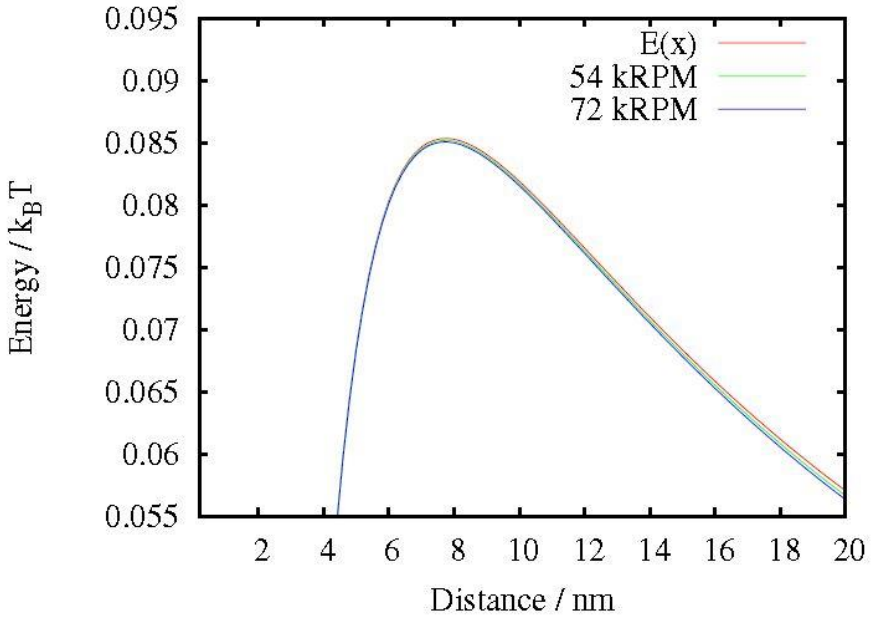

Figure 3.12: Energy landscape of E trimer-membrane bond interface as a function of distance away from the membrane. The effects of centrifugal force at 54,000 and 72,000rpm are negligible and do not lower the energy barrier. Figure adapted from [44].

Another force that may affect protein-membrane unbinding is shear force generated by flow as liposomes migrate upward through the sucrose environment. Shear force calculations were made according to Equation 3.2.

$$F_{drag} = k_B T \frac{v}{D} \qquad \text{Equation 3.2}$$

where F_{drag} is the force on a protein moving at a given velocity through the sucrose environment, k_B is the Boltzmann constant, T is temperature, v is particle velocity (based on the sucrose viscosity and average vesicle diameter), and D is the diffusion coefficient for soluble E trimer. For a diffusion coefficient of $3x10^{-7}$ cm^2/s (Stokes radius of 8nm), a velocity of ~0.05mm/min for a trimer in the sucrose gradient at 54,000rpm (calculated from the Svedberg equation) [44], and temperature of 4°C, the drag force experienced by a trimer is roughly $1x10^{-4}$pN. This force also appears to be too small to affect the energy barrier for unbinding. Coflotation results for PC:PE at 27,000rpm for 2.75hr from Figure 3.10 reinforces that centrifugal and shear forces do not appear to have an effect on unbinding. At a lower rotor speed of 27,000rpm, the centrifugal and shear forces are lower; however, protein is still not detected in the top fractions under these conditions.

A third possibility is that centrifugation and coflotation probe the rate of protein unbinding from the membrane, which is determined by the energy barrier relative to k_BT. As natural dynamics occur for the protein/membrane system, the position of E within the membrane will fluctuate and occasionally protein molecules will pass over the energy

barrier and move to the very edge of the membrane. Under centrifugation as E unbinds from the membrane, it experiences a centrifugal force that pulls it away from the membrane toward lower fractions of the gradient. This rapid removal of E molecules that have moved to the edge of the membrane by virtue of thermal fluctuations will accelerate the rate of unbinding as they are unable to equilibrate with and reinsert into the membrane. The energy requirement for E to unbind from PC:PE membranes is lower compared to PC:PG due to weaker anchoring in the membrane, thus we expect the energy barrier to be crossed more frequently and centrifugation to have a greater accelerating effect on the rate of unbinding for PC:PE. Since the anchoring energy of E in PC:PG membranes is greater, the off-rate is much slower and centrifugation has a small effect on the rate of unbinding in that case.

In the QCM measurements, after the final addition of E had approached steady state, pure buffer was flowed through the sample chamber. Upon flowing buffer though the chamber there was a gradual increase in frequency for the case of PC:PE, but the frequency did not increase for PC:PG. This suggests that E was gradually unbinding from the PC:PE membrane but not from the PC:PG membrane. We suggest that this reflects the difference in natural off-rate mentioned above, and that given enough time E would entirely unbind in this system as was observed in the coflotation assay. However, centrifugation accelerates the effect such that it can be observed on a practical time scale.

Considering this hypothesized mechanism we now return to the coflotation results for reduced speed and centrifugation time in Figure 3.10. The results show more protein was observed in the middle fractions at the lower spin time of 1hr but maximum speed of 54,000rpm, whereas no protein was observed in the middle or top portions of the gradient

at lower rotor speed of 27,000rpm and 2.75hr. Regarding the results for reduced spinning time at 54,000rpm, more protein is found in the middle of the gradient because in that case the time was insufficient for the protein to migrate to the bottom of the gradient. Regarding the result at lower rotor speed but a time of 2.75hrs, we suggest that a lower rotor speed applied over the same length of time caused liposomes to migrate upward more slowly, yet the speed was still sufficient for sedimentation of protein that unbound from the membrane. Since the liposome/protein solution was deposited near the bottom portion of the gradient and the rate of liposome flotation was reduced, the protein came off the membrane while the liposomes were in the lower or middle portions of the gradient and had less distance to sediment back to the bottom of the gradient. Thus, no protein is seen in the top or middle fractions.

Lastly, we consider whether differences in E anchoring are a function of inadequate protein coverage for PC:PE membranes. Figure 3.6 demonstrates that at 6μM the amount of E adsorbed to PC:PE membranes is greater than the amount adsorbed to PC:PG membranes at 1μM. Yet coflotation experiments demonstrate a far greater rate of protein unbinding from PC:PE membranes even at higher coverage (Figure 3.9). This demonstrates that the differences in membrane unbinding are independent of protein coverage, confirming that protein anchoring to the membrane is greater with anionic lipids.

3.5 Chapter Summary

QCM and coflotation studies were conducted to examine the differences in E protein binding and anchoring to PC:PG and PC:PE membranes. Binding curves by QCM showed that for both lipid compositions adsorption of E is detectable at 0.1μM, and that the binding affinity is higher for PC:PG than for PC:PE. Most importantly, at 6μM the amount of E adsorbed to PC:PE membranes is greater than that adsorbed to PC:PG membranes at 1μM. The coflotation assay showed that for PC:PE membranes, E unbound as a function of time under the influence of centrifugal force, even at high coverage of 6μM, whereas little unbinding of E was detected for PC:PG membranes at lower coverage, even after 25hrs. This demonstrates that PC:PG membranes afforded greater E anchoring. While other studies have shown that E adsorbs and inserts into membranes lacking anionic lipids [3, 8, 14], prior to the present work it was not known if the anchoring energy in that case is sufficient to support membrane fusion. The present work has shown that for neutral membranes the anchoring energy is substantially lower than for membranes with anionic lipids and is likely to be inadequate to support membrane fusion.

It was concluded that centrifugal forces and shear forces from coflotation experiments are not large enough to affect the protein-membrane binding interaction; however, coflotation is able to probe the off-rate of protein binding by pulling protein away from the membrane after it unbinds. Thus, coflotation assays give insight into the anchoring of E to each membrane type by measuring protein unbinding. The greater rate of unbinding indicates that the anchoring energy is lower for PC:PE membranes, and the lower anchoring energy likely explains why fusion does not occur in the absence of

negatively-charged lipids. This methodology provides the capability to probe protein anchoring energy for weaker interacting systems than can be studied by AFM.

Chapter 4

E PROTEIN OLIGOMERIZATION DEPENDENT UPON TARGET MEMBRANE CHARGE

4.1 Introduction

The formation of E protein trimers is believed necessary for flavivirus membrane fusion [5, 8, 32-36, 42]. While this requirement has been widely accepted based on the ubiquitous finding of trimers in crystallization studies of membrane-bound E at low pH [8, 14], the specific events leading up to final trimer assembly are not fully understood. The formation of fusogenic trimers depends upon specific environmental factors. One is pH and low pH exposure in the endosome, triggering the rearrangement of native dimers into E trimers, as described in Chapter 1 Section 1.2. In addition to an acidic environment, it has also been shown that for tick-borne encephalitis virus (TBEV), the presence of a target lipid membrane is another environmental factor required for trimerization. When E dimers were exposed to low pH in the absence of a membrane, they reversibly dissociated into monomers, but did not form trimers [37]. Furthermore, target membrane binding of TBEV has been shown to occur only via the intermediate monomeric form of E [38], so it can be concluded that target membrane binding facilitates trimerization. The importance of the target membrane in TBEV trimer formation suggests a similar role may also exist in the trimerization of other flaviviruses like DENV.

In addition to the presence of a target membrane, several studies have further investigated the effect of lipid membrane composition. Specifically, TBEV studies revealed that increased binding and trimerization of E protein occurred due to the

presence of cholesterol and sphingomyelin in the membrane [27]. A similar study for DENV investigated the role of cholesterol in the membrane; however, unlike TBEV, cholesterol did not promote efficient DENV membrane fusion, but rather only promoted the initial E protein-membrane interaction [22]. We note that the latter study involved membranes lacking anionic lipids.

Another important aspect of membrane composition that may affect the overall extent of trimerization is the charge of the phospholipid head groups comprising the membrane. DENV fusion has been shown to only occur with membranes containing anionic lipids [13]; however, exactly how these lipids facilitate fusion remains unknown. One hypothesis is that membrane charge promotes oligomerization of monomers into fusogenic trimers, analogous to the hypothesized role of cholesterol in facilitating trimer formation in alphaviruses [22, 48]. Trimerization could promote negative curvature within the membrane. In addition, trimerization would substantially increase membrane anchoring. Indeed, others have proposed that a single fusion loop would not be sufficient for a stable membrane interaction but that trimers are required [22]. Here, we begin to examine how the presence of anionic lipids affects the oligomeric state of E protein bound to the membrane. The studies performed have included sucrose gradient sedimentation to separate various oligomeric states and analyze the amount of trimer that forms in the presence of negatively-charged and neutral membranes. Magnetic beads were used to remove lipid and detergent residues from samples prior to sedimentation to better resolve each oligomeric state within the sucrose gradient. Chemical crosslinking was used as an alternative technique to detect trimer formation in the presence of the

various membrane compositions. Additional work will be needed to fully understand how trimer assembly is facilitated by negative charge in the membrane.

4.2 Experimental Section

4.2.1 Materials and Methods

4.2.1.1 Liposome Preparation

70:30 POPC:POPE, 70:30 POPC:POPG, and a third liposome composition containing 1:1:1:3 molar ratio of POPC, POPE, sphingomyelin, and cholesterol were made according to the protocol described in Chapter 2. 2-3mg/ml stock solutions of sphingomyelin (chicken egg yolk) (Sigma-Aldrich) and cholesterol (Avanti) were made in 9:1 solution of chloroform and methanol and incorporated into the liposome mixture according to the prescribed molar ratio. Lipids were dried overnight and rehydrated with TAN buffer pH 8.0. 10 freeze/thaw cycles were followed by 21-pass extrusion through a 200nm membrane. Liposomes were stored at 4˚C and used within two weeks of preparation.

4.2.1.2 Sucrose Gradient Sedimentation of E Oligomers

Velocity sedimentation assays were performed to examine the oligomeric state of E protein upon binding to liposomes of different compositions. A solution of 1μM sE combined with 1mM liposomes was acidified with a pre-calibrated volume of 0.3M MES buffer, pH 0.61 and allowed to incubate at pH 5.5 for 30min. Samples were then back neutralized to pH 8.0 with a pre-calibrated amount of 0.3M TEA buffer, pH 12.5. Once

trimers form, they have been shown to be stable, even after back neutralization [38]. To solubilize membrane-bound protein from the liposomes, 1.5% octyl β-D-glucopyranoside (n-OG) (Sigma) was added to the reaction mixture. In accordance with previous protocols, the samples were vortexed to thoroughly mix and then incubated at 25°C for 60min [27, 33]. The samples were then deposited on a sucrose sedimentation gradient for analysis.

Sucrose sedimentation gradients were made in Beckman Ultra-Clear 5mm x 41mm centrifuge tubes in a total volume of 700µl. The volume ratio for each layer was adapted from [14] and adjusted to the smaller volume. Figure 4.1 shows a schematic of the gradient layers, along with the corresponding volumes, and sample placement before centrifugation. 100µl of 40% sucrose in TAN was overlaid by 200µl of 20% sucrose followed by 200µl of 10% sucrose. 100µl of 5% sucrose in TAN was deposited over the 15% layer, and the solubilized liposome-protein sample (100µl) was deposited at the top of the gradient. 1% n-OG was included in each gradient layer. Gradients were subject to centrifugation for 6hr 15min at 54,000rpm at 4˚C using a Beckman SW55Ti rotor [3, 14, 17]. Figure 4.1 demonstrates the ideal separation of the various oligomeric states resolved according to their sedimentation velocity. 35µl fractions were collected from the gradient by hand using a glass syringe. A total of 20 fractions were collected, consistent with the 700µl total volume.

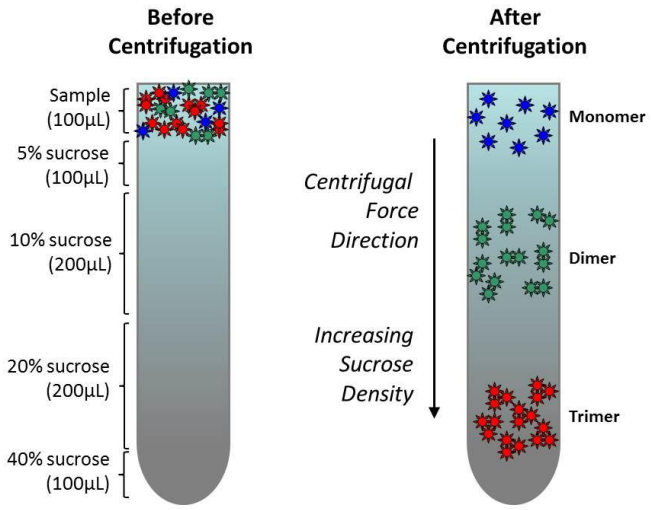

Figure 4.1: Schematic of sedimentation gradient: Acidified protein-liposome reaction mixtures were mixed with n-OG after incubation, solubilizing the liposomes. The mixture was deposited on top of the gradient. Upon centrifugation, the various E protein oligomers separated according to the differences in sedimentation velocity for monomer, dimer, and trimer.

4.2.1.3 Magnetic Bead Separation

Magnetic bead separation was used to isolate E oligomers from solubilized lipid and n-OG detergent. *Strep*-Tactin Magnetic Beads (QIAGEN, Germany) were added to back neutralized protein-lipid solutions in a ratio of 10µl of bead solution for every 1µg of protein in the sample. Samples were gently mixed for 60min while incubated at 4°C. Beads were separated from the supernatant and washed twice with NP-T buffer (50mM NaH_2PO_4, 300mM NaCl, 0.05% Tween 20, pH 8.0) to remove lipid and n-OG residue. E protein was recovered by the addition of 50µl NPB-T buffer (50mM NaH_2PO_4, 300mM NaCl, 10mM biotin, 0.05% Tween 20, pH 8.0) added to the beads and incubated for 5min

at 37°C. NPB-T rinses were carried out four times for a total eluate of 200µl. 100µl of the eluate was deposited on the sedimentation gradient for analysis.

4.2.1.4 Chemical Crosslinking

In addition to sedimentation, chemical crosslinking was used to capture the oligomeric state of E protein after low pH exposure in the presence of liposomes. The top three fractions of coflotation gradients with 1:1:1:3 (PC:PE:sphingomyelin:chol) liposomes were back neutralized to pH 8.0 before adding dimethyl suberimidate (DMS) (Thermo Scientific) dissolved in crosslinking buffer (0.2M triethanolamine, pH 8.0) to a final concentration of 0.5mM. DMS is a membrane-permeable crosslinker containing an amine-reactive imidoester group. Crosslinking proceeded for 30min at 25°C and was terminated by the addition of Tris HCl to a final concentration of 20mM. Samples were incubated for 15min to fully stop the reaction before further analysis by SDS-PAGE.

4.3 Results

4.3.1 Resolving Individual Oligomeric States

Samples of E protein and PC:PG or PC:PE liposomes incubated at pH 5.5 were analyzed by sucrose gradient sedimentation to resolve the amount of trimer formed in the presence of each membrane type. After incubation, E protein was solubilized from the liposomes and the mixture was deposited on the gradient and centrifuged. The various E oligomers separated within the gradient according to their size. Analyzing the collected fractions revealed where E migrated within the gradient, and SDS-PAGE qualitatively

indicated the relative amount of monomer, dimer, and trimer according to the observed protein band intensity. As shown in Figure 4.2, band intensity appears to shift more towards the bottom fractions in the case of PC:PG liposomes compared to PC:PE. E protein alone at pH 5.5 appears to have a peak in band intensity approximately at Fraction 5, while E protein alone at pH 8.0 has a peak around Fraction 7. The observed protein spreading throughout the gradient is largely due to the presence of n-OG within the reaction sample and the gradient, making the identification of peak positions more challenging.

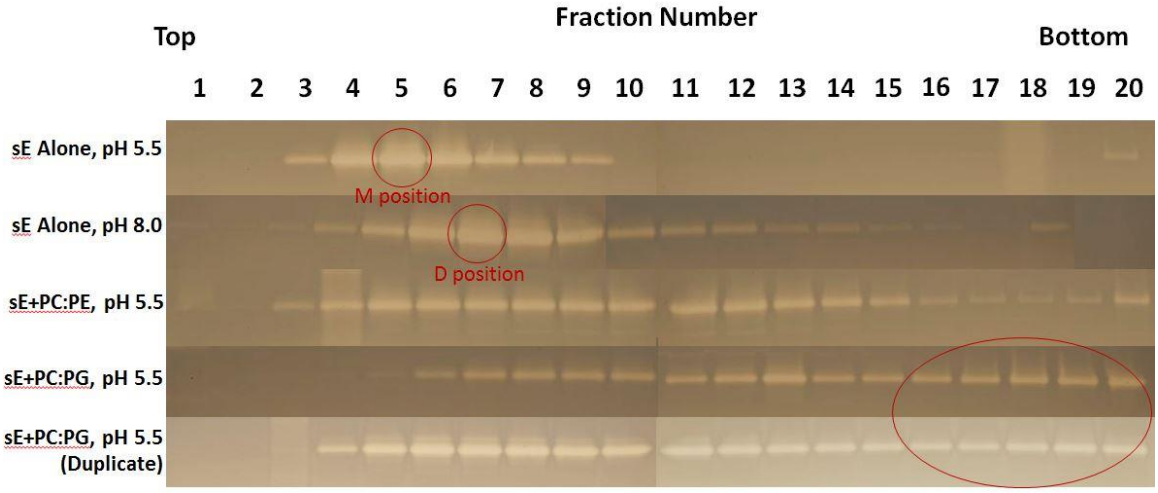

Figure 4.2: Sedimentation of sE alone, sE+PC:PG, and sE+PC:PE: Controls of sE alone at pH 5.5 and 8.0 demonstrate where monomeric and dimeric E migrates within the gradient. The shift in protein content towards the bottom of the gradient for PC:PG may indicate where trimers sediment. Increased amount of E found near the bottom of the gradient when mixed with PC:PG liposomes compared to PC:PE suggests an increase in trimer formation in the presence of anionic lipids.

Further sedimentation studies of DENV E were conducted with liposomes comprised of a 1:1:1:3 ratio of POPC, POPE, sphingomyelin, and cholesterol. With this composition, others reported that 50% of E protein bound to these membranes, and nearly all the protein bound was identified as trimer [14]. Sedimentation assays were conducted with 1:1:1:3 liposomes as a positive control of trimer formation to compare with results obtained for PC:PG and PC:PE systems. In addition, sedimentation experiments with these liposomes were done without n-OG so that oligomer peaks could be more easily identified. Results of this experiment are shown in Figure 4.3. E protein alone was acidified to create monomers and deposited on a gradient maintained at pH 5.5. In the absence of a membrane, the monomers remained soluble and sedimented near the top of the gradient, with a peak position centered near Fraction 5. To identify the location of dimers, E protein alone at pH 8.0 was deposited on a gradient maintained at neutral pH, revealing a peak centered at Fraction 6. Lastly, in an attempt to identify E protein trimers, the reaction mixture was separated from the lipid membranes and n-OG by magnetic bead separation before being applied to the gradient. Though trimers were not solely isolated by this technique, their formation was still detectable in reference to the location of monomer and dimer peaks.

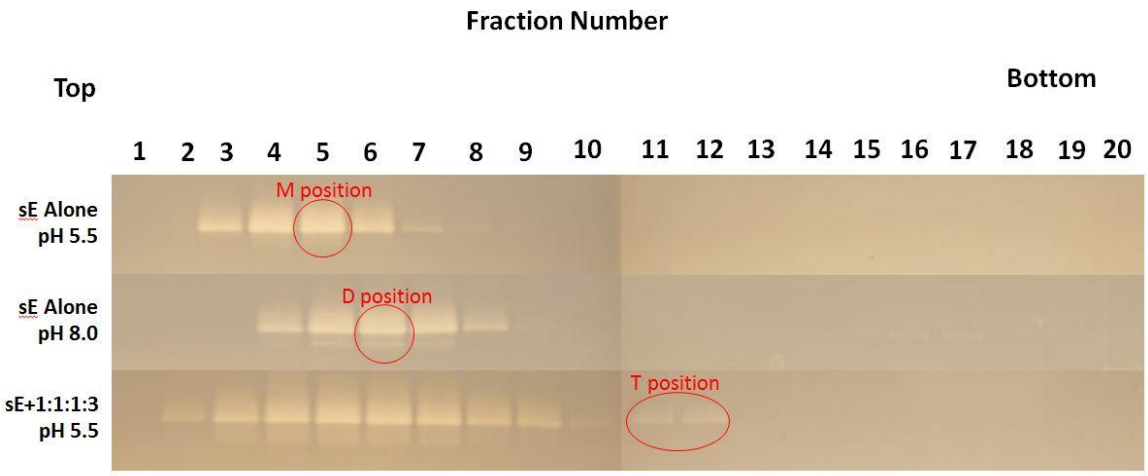

Figure 4.3: Sedimentation of isolated oligomeric states without n-OG: Acidified E alone identifies E monomers sediment at approximately Fraction 5. E alone maintained at pH 8.0 revealed dimer sedimented around Fraction 6. E oligomers from protein-liposome reaction mixtures (1:1:1:3 liposomes) were separated from lipids and n-OG before sedimentation. In this case, E found in Fractions 11 and 12 provides evidence of trimer formation in relation to the peak monomer and dimer positions.

4.3.2 Identifying Oligomeric States by Crosslinking

Chemical crosslinking was also used to identify the oligomeric state of E protein. 1:1:1:3 liposomes were again used as a positive control for trimer formation, to compare with results of PC:PG and PC:PE experiments. However, instead of using the entire reaction mixture of E protein and liposomes, coflotation was first conducted to separate membrane-bound from unbound E protein. Then, the top three fractions of the gradient were collected and each was crosslinked according to the protocol described above. The

crosslinked samples were then analyzed to reveal the relative amounts of each oligomer present. The results demonstrate that in each of the three fractions, monomer was predominantly found, followed by lesser amounts of dimer, and only trace amounts of trimer.

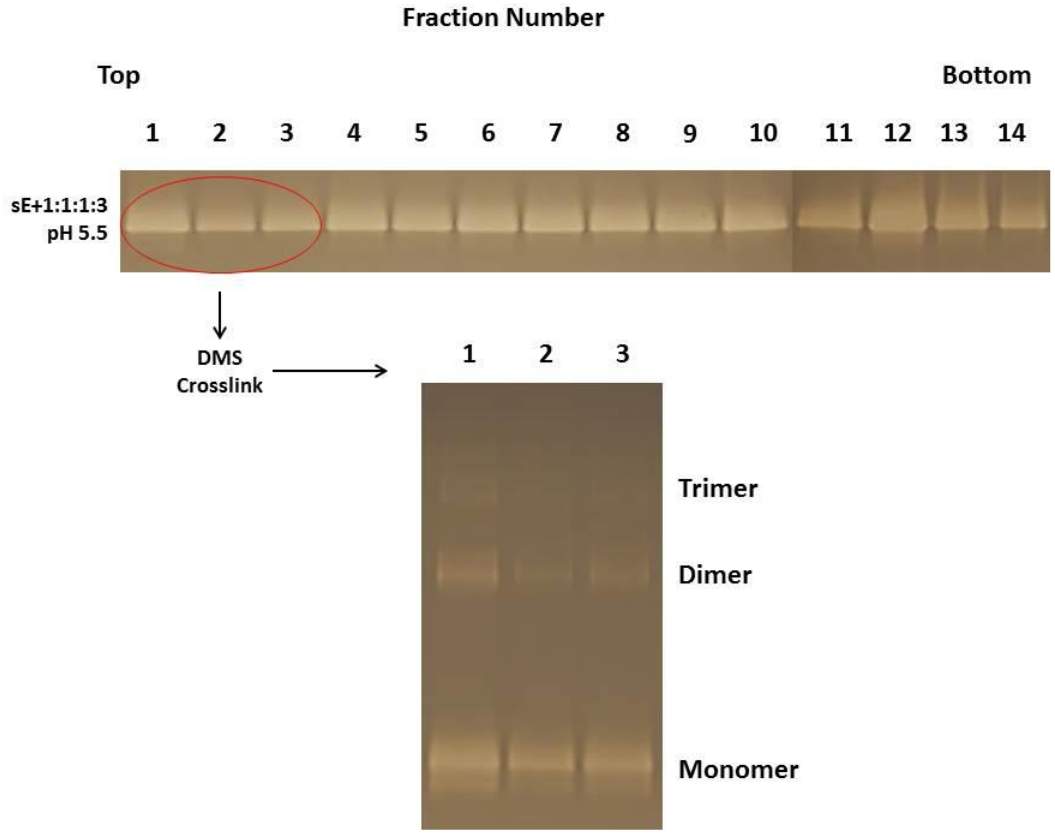

Figure 4.4: Coflotation of 1:1:1:3 liposomes followed by crosslinking: The top three fractions from coflotation were DMS crosslinked and analyzed by SDS-PAGE. A majority of the crosslinked E in these fractions appears monomeric with some dimer also present. Only trace amounts of trimer can be seen in Fraction 1, revealing far less trimerization in the membrane-bound state than anticipated.

4.4 Discussion

4.4.1 Sucrose Gradient Sedimentation

Sedimentation of E protein monomer, dimer, and trimer by gradient centrifugation is achieved by the differences in individual sedimentation velocities of each oligomer. The rate of oligomer sedimentation is dictated by the size and mass of the molecules, as opposed to molecular density. As such, sedimentation of trimers is most rapid, migrating to lower fractions of the gradient, while monomers sediment most slowly and remain closest to the top. Greater protein band intensity in lower fractions of the gradient for PC:PG liposomes compared to PC:PE liposomes indicates a qualitative difference in the amount of trimer formed. Thus, the results in Figure 4.2 suggest that trimer formation is increased due to the presence of anionic lipids in the target membrane. However, fully resolving individual oligomeric states is challenging from these data due to the spreading effects caused by detergent in the gradient. The small diameter centrifuge tubes used in this assay along with the hydrophobic tube material made fraction collection of n-OG solubilized samples difficult due to capillary action in the centrifuge tube. But, a qualitative shift in protein content to lower fractions in the case of PC:PG liposomes is clearly evident. Based on this observation, anionic lipids appear to encourage a greater extent of oligomerization, presumably trimerization, compared to PC:PE membranes.

The experiments described above indicate that the presence of PC:PG membranes leads to an increase in E protein oligomers of size greater than dimers. However, the mixture of oligomeric states and the presence of detergent are both complicating factors. An important experiment necessary to further understand if anionic lipids encourage

trimerization will be to isolate and quantify the oligomeric states of only membrane-bound E for both PC:PE and PC:PG membranes. Coflotation experiments from Chapter 2 revealed that E anchoring energy is greatly enhanced by negatively-charged membranes, but E binding still occurs to some extent with PC:PE membranes. Identifying the oligomeric state of E bound to PC:PE compared to PC:PG will help elucidate the role of anionic lipids during trimerization. Additionally, these experiments will also afford greater understanding of the observed differences in anchoring energy, which may be a result of differences in the oligomeric states.

Figure 4.3 depicts the subtle differences in monomer and dimer sedimentation, with peak positions of each appearing near the top of the gradient, only one or two fractions from each other. In the presence of 1:1:1:3 liposomes, a faint trimer peak appears in later fractions towards the middle of the gradient. Interestingly, though 1:1:1:3 liposomes were used to encourage trimer formation, only a small amount of trimer seems to be detectable. No anionic lipids are present in the 1:1:1:3 membranes, which may be the reason why trimer formation appears to be minimal. However, other reports utilizing very similar protocols and the same membrane composition [3, 14] have reported much greater trimer formation than what is observed here. Further studies are needed to resolve this discrepancy and increase trimer formation before examining PC:PG and PC:PE systems.

4.4.2 Chemical Crosslinking

In addition to sedimentation gradients, chemical crosslinking was another strategy used to identify the oligomeric state of E protein. Various concentrations of DMS were

examined to optimize crosslinking without generating large amounts of protein aggregates (data not shown). 0.5mM DMS demonstrated a reasonable amount of crosslinking efficiency and did not cause excessive protein aggregation. Coflotation analysis involving a solution of sE incubated with 1:1:1:3 liposomes resulted in a distribution of protein in all fractions of the gradient. This result indicates an anchoring energy of sE in the membrane that is intermediate between that for PC:PG liposomes and PC:PE liposomes. This is consistent with a prior study that showed cholesterol increased the binding of sE to membranes lacking anionic lipids [22]. When cofloating fractions were crosslinked at 0.5mM DMS, only a small amount of trimer was detected in relation to the other oligomers, as shown in Figure 4.4. However, some question remains regarding the efficiency of the crosslinking reaction at 0.5mM DMS. Other studies have shown that crosslinking is inefficient, and that even when the majority of the sample is in trimer form, crosslinking followed by SDS-PAGE analysis results in most of the protein running as a monomer and dimer, and only a minority of the sample running as a trimer [33, 38, 42, 47]. Recognizing that crosslinking is somewhat efficient, it is still interesting to compare this apparent low trimerization result with the data in Figure 4.3 where a similar effect was observed. More experimentation is required to further understand this issue of low trimer formation in experiments involving magnetic bead separation or in crosslinking experiments before these methods could be applied to mitigate the experimental difficulties induced by the use of detergent in the original sedimentation experiments shown in Figure 4.2.

4.5 Chapter Summary

The effect anionic lipids in the target membrane have on the extent of trimer formation was examined by sucrose gradient sedimentation and chemical crosslinking. Sedimentation of E incubated with either PC:PE or PC:PG liposomes at pH 5.5 revealed an overall increase in protein intensity in the bottom fractions of the gradient for the case of PC:PG, suggesting greater trimer (and possibly higher order oligomer) formation. Though some trimer appeared for the case of PC:PE, the shift in intensity suggests that anionic lipids are able to encourage a greater extent of trimerization. The individual oligomeric states, isolated from lipid and detergent, were examined by sedimentation and peak positions of monomer, dimer, and trimer were identified. These control measurements afforded better resolution to each oligomer that would otherwise be difficult to achieve from a mixture of the three due to fraction overlap.

Chemical crosslinking was used as another method to identify the oligomeric state of membrane-bound E protein obtained from the top three fractions after coflotation with 1:1:1:3 liposomes. Only trace amounts of trimer were identified as membrane-bound, while a majority of the protein was identified as monomer and dimer. This is further evidence suggesting that anionic lipids are required to induce trimerization; however, other groups reported significant trimerization using the same liposome composition [3, 8, 14, 46]. The source of this discrepancy is not yet clear.

Much additional work remains to resolve trimer yield before further detailed comparisons between PC:PE and PC:PG membranes can be made to elucidate the full role of anionic lipids in facilitating trimerization.

Chapter 5

CONCLUSIONS AND RECOMMENDATIONS FOR FUTURE WORK

5.1 Conclusions

5.1.1 E Protein Anchoring

Coflotation was utilized as a method to probe E protein unbinding from PC:PG and PC:PE membranes. As this method is further developed, it will serve as an important technique to probe protein-membrane unbinding, which currently is mainly measured by AFM. Coflotation is more sensitive to detect unbinding of weaker protein interactions with the membrane, making it particularly useful for examining the unbinding of E trimers from liposome membranes. Coflotation revealed that membrane unbinding occurs at a much lower rate from PC:PG liposomes, demonstrating that the anchoring energy of E into membranes containing anionic lipids is much greater compared to PC:PE where no anionic lipids are present. Sufficient anchoring is crucial to successful membrane fusion because the binding interaction must withstand the large energies associated with membrane bending. Thus, the results from this study provide a fundamental biophysical explanation of the anionic lipid requirement for fusion that was reported in previous studies. Though additional work will further elucidate the effect anionic lipids have on DENV fusion, the work presented here reveals key insight into their function of membrane anchoring.

5.1.2 E Protein Oligomerization

Sucrose gradient sedimentation was utilized to separate the individual oligomeric states of E protein after incubation with PC:PG and PC:PE liposomes. The data revealed

a qualitative shift in protein band intensity towards the bottom fractions of the gradient, suggesting increased trimer formation (and possibly higher order oligomers) occurred in the presence of anionic lipids. Chemical crosslinking with liposomes containing cholesterol, but lacking anionic lipids revealed only a small extent of trimer formation. This may reveal that anionic lipids are required for trimerization; however, other studies reported much higher trimer formation with the same liposome composition. Further work is necessary to refine both chemical crosslinking and sedimentation assays. Though full understanding of how anionic lipids affect the oligomerization of E has not been achieved, an important foundation for further examination of this effect has been established.

5.2 Future Work

Gel staining techniques were used for protein detection in coflotation and sedimentation studies; however, more quantitative measurement techniques should be used to further support the findings of this work. For studies of E oligomerization, fluorescently labeling E protein in each sedimentation fraction will more accurately resolve the peak position of each oligomer. This technique will also clearly reveal quantitative differences in the amount of each oligomer formed in the presence of PC:PG versus PC:PE membranes.

Further studies investigating how membrane composition affects E anchoring and oligomerization will be very useful in elucidating the fusion mechanism. The addition of cholesterol and sphingomyelin to target membranes are essential factors in the fusion of

alphaviruses [17, 48], and cholesterol has been shown to facilitate fusion for some flaviviruses [27] but not others [22]. We propose further studies with membranes containing cholesterol, sphingomyelin, and anionic lipids. Prior studies have already examined the effect of cholesterol in DENV fusion, finding it was not essential to trimerization, but promoted membrane binding in the absence of anionic lipids [22]. We believe that both cholesterol and anionic lipids may be required for efficient trimer formation. Cholesterol may facilitate monomer insertion into the target membrane while anionic lipids may facilitate trimerization.

Additional membrane composition studies exchanging POPG for POPS lipids will also be valuable in future studies. Molecular dynamics simulations have suggested that the lower area per lipid molecule afforded by anionic lipids in PC:PG liposomes may facilitate increased anchoring of E. This hypothesis could be tested by repeating the coflotation experiments with liposomes composed of 70:30 PC:PS. Such membranes would have negative charge, but a different packing density as the area per molecule is known to differ for PG versus PS. Studies with such liposomes would reveal whether lipid packing affects anchoring or whether anchoring is solely dependent upon charge.

Finally, while the present work shows that the coflotation methodology developed here is highly sensitive to differences in anchoring energy, the quantitative values for the energy barriers associated with unbinding were not obtained. It may be possible in some cases to determine the energy barriers for unbinding through more extensive coflotation/sedimentation studies that measure the unbinding kinetics as a function of time and temperature coupled with modeling of first passage times. In addition, it would be useful to compare the rates of unbinding by the coflotation/sedimentation methods to

those obtained with QCM under conditions of constant flow of buffer through the sample chamber. Flow of buffer through the QCM cell may accomplish the same effect in removing protein from the membrane region as is postulated to occur by centrifugation in the coflotation assay.

REFERENCES

1. Acosta E.G., Talarico L.B., Damonte E.B. Cell entry of dengue virus. *Future Virol*, 2008. 3(5): 471-479.

2. Rodenhuis-Zybert I., Wilschut J., Smit J.M. Dengue virus life-cycle: viral and host factors modulating infectivity. *Cell Mol Life Sci*, 2010. 67:2773-2786.

3. Zheng A., Umashankar M., Kielian M. In vitro and in vivo studies identify important features of dengue virus pr-E protein interactions. *PLoS Path*, 2010. 6(10): 1-12.

4. Kyle J.L., Harris E. Global Spread and Persistence of Dengue. *Annu Rev Microbiol*, 2008. 62: 71-92.

5. Sánchez-San Martín C., Liu C.Y., Kielian M. Dealing with low pH: entry and exit of alphaviruses and flaviviruses. *Trends in Microbiol*, 2009. 17(11): 514-520.

6. Halstead S.B. Dengue. *Lancet*, 2007. 370(9599): 1644-1652.

7. WHO. Dengue and dengue haemorrhagic fever. *WHO Fact Sheet117*, 2012. WHO, Geneva Switzerland.

8. Modis Y., Ogata S., Clements D., Harrison S.C. Structure of the dengue virus envelope protein after membrane fusion. *Nature*, 2004. 427:313-319.

9. Muñoz M.L., Cisneros A., Cruz J., Das P., Tovar R., Ortega A. Putative dengue virus receptors from mosquito cells. *FEMS Microbio. Lett*, 1998. 168: 251-258.

10. Chee H-Y., AbuBakar S. Identification of a 48 kDa tubulin or tubulin-like C6/36 mosquito cells protein that binds dengue virus 2 using mass spectroscopy. *Biochem Biophys Res Commun*, 2004. 320: 11-17.

11. Wei H.Y., Jiang L.F., Fang D.Y., Guo H.Y. Dengue virus type 2 infects human endothelial cells through binding the viral envelope glycoprotein to the cell surface polypeptides. *J Gen Virol*, 2003. 84: 3095-3098.

12. Lindenbach B.D., Thiel H-J., Rice C.M. Flaviviruses: the viruses and their replication. In: Knipe D.M., Howley P.M., eds. Fields Virology 5th Ed. 2007. Philadelphia: Lippincott, Williams, and Wilkins. pp. 1101-1152.

13. Zaitseva E., Yang S.T., Melikov K., Pourmal S., Chernomordik L.V. Dengue virus ensures its fusion in late endosomes using compartment-specific lipids. *PLoS Path*, 2010. 6(10): 1-14.

14. Liao M., Sánchez-San Martín C., Zheng A., Kielian M. In vitro reconstitution reveals key intermediate states of trimer formation by the dengue virus membrane fusion protein. *J Virol*, 2010. 84(11): 5730-5740.

15. Melo M.N., Sousa F.J.R., Carneiro F.A., Castanho M.A.R.B., Valente A.P., Almeida F.C.L., Da Poian A.T., Mohana-Borges R. Interaction of the dengue virus fusion peptide with membranes assessed by NMR: The essential role of the envelope protein Trp101 for membrane fusion. *J Mol Biol*, 2009. 392: 736-746.

16. Perera R., Khaliq M., Kuhn R.J. Closing the door on flaviviruses: Entry as a target for antiviral drug design. *Antiviral Research*, 2008. 80: 11-22.

17. Sánchez-San Martín C., Sosa H., Kielian M. A stable prefusion intermediate of the alphavirus fusion protein reveals critical features of class II membrane fusion. *Cell Host and Microbe*, 2008. 4: 600-608.

18. Harrison S.C. Viral membrane fusion. *Nat Struct Mol Biol*, 2008. 15(7): 690-698.

19. Halstead S.B. Observations related to pathogenesis of dengue hemorrhagic fever. VI. Hypothesis and discussion. *Yale J Biol and Med*, 1970. 42: 350-362.

20. Perera R., Kuhn R.J. Structural proteomics of dengue virus. *Curr Opinion Microbio*, 2008. 11: 369-377.

21. Yu I-M., Zhang W., Holdaway H.A., Li L., Kostyuchenko V.A., Chipman P..R., Kuhn R.J., Rossmann M.G., Chen J. Structure of immature dengue virus at low pH primes proteolytic maturation. *Science*, 2008. 319: 1834-1837.

22. Umashankar M., Sánchez-San Martín C., Liao M., Reilly B., Guo A., Taylor G., Kielian M. Differential cholesterol binding by class II fusion proteins determines membrane fusion properties. *J Virol*, 2008. 82(18): 9245-9253.

23. Gregoriadis G. Liposome technology: entrapment of drugs and other materials. Vol II. 2nd Ed. 1993. Boca Raton: CRC Press, Inc. pp. 77-79.

24. Hope M.J., Bally M.B., Webb G., Cullis P.R. Production of large unilamellar vesicles by a rapid extrusion procedure: characterization of size distribution, trapped volume and ability to maintain a membrane potential. *Biochim Biophys Acta*, 1985. 812(1): 55-65.

25. Hupfeld S., Moen H.H., Ausbacher D., Haas H., Brandl M. Liposome fractionation and size analysis by asymmetrical flow field-flow fractionation/multi-angle light scattering: influence of ionic strength and osmotic pressure of the carrier liquid. *Chem and Phys of Lipids*, 2010. 163(2): 141-147.

26. Lasic D.D. Novel applications of liposomes. *Tibtech*, 1998. 16: 307-321.

27. Stiasny K., Koessl C., Heinz F.X. Involvement of lipids in different steps of the flavivirus fusion mechanism. *J Virol*, 2003. 77(14): 7856-7862.

28. Stiasny K., Heinz F.X. Flavivirus membrane fusion. *J Gen Virol*, 2006. 87: 2755-2766.

29. Kuhn R.J., Zhang W., Rossmann M.G., Pletnev S.V., Corver J., Lenches E., Jones C.T., Mukhopadhyay S., Chipman P.R., Strauss E.G., Baker T.S., Strauss J.H. Structure of dengue virus: implications for flavivirus organization, maturation, and fusion. *Cell*, 2002. 108: 717-725.

30. Weissenhorn W., Dessen A., Calder L.J., Harrison S.C., Skehel J.J., Wiley D.C. Structural basis for membrane fusion by enveloped viruses. *Mol Membr Biol*, 1999. 16: 3-9.

31. Stiasny K., Allison S.L., Mandl C.W., Heinz F.X. Role of metastability and acidic pH in membrane fusion by tick-borne encephalitis virus. *J Virol*, 2001. 75(16): 7392-7398.

32. Hernandez L.D., Hoffman L.R., Wolfsberg T.G., White J.M. Virus-cell and cell-cell fusion. *Annu Rev Cell Dev Biol*, 1996. 12: 627-661.

33. Stiasny K., Bressanelli S., Lepault J., Rey F.A., Heinz F.X. Characterization of a membrane-associated trimeric low-pH-induced form of the class II viral fusion protein E from tick-borne encephalitis virus and its crystallization. *J Virol*, 2004. 78(6): 3178-3183.

34. White J.M. Viral and cellular membrane fusion proteins. *Annu Rev Physiol*, 1990. 52: 675-697.

35. Gaudin Y., Ruigrok R.W.H., Brunner J. Low-pH induced conformational changes in viral fusion proteins: implications for the fusion mechanism. *J Gen Virol*, 1995.

76: 1541-1556.

36. Fritz R., Blazevic J., Taucher C., Pangerl K., Heinz F.X., Stiasny K. Unique transmembrane hairpin of flavivirus fusion protein E is essential for membrane fusion. *J Virol*, 2011. 85(9): 4377-4385.

37. Stiasny K., Allison S.L., Marchler-Bauer A., Kunz C., Heinz F.X. Structural requirements for low-pH-induced rearrangements in the envelope glycoprotein of tick-borne encephalitis virus. *J Virol*, 1996. 70(11): 8142-8147.

38. Stiasny K., Allison S.L., Schalich J., Heinz F.X. Membrane interactions of the tick-borne encephalitis virus fusion protein E at low pH. *J Virol*, 2002. 76(8): 3784-3790.

39. Winterhalter M., Lasic D.D. Liposome stability and formation: experimental parameters and theories on the size distribution. *Chem Phys Lipids*, 1993. 64: 35-43.

40. Laue T.M., Stafford W.F. Modern applications of analytical ultracentrifugation. *Annu Rev Biophys Biomol Struct*, 1999. 28: 75-100.

41. Yadav A.V., Murthy M.S., Shete A.S., Sakhare S. Stability Aspects of Liposomes. *Ind J Pharm Edu Res*, 2011. 45(4): 402-413.

42. Allison S.L., Schalich J., Stiasny K., Mandl C.W., Kunz C., Heinz F.X. Oligomeric rearrangement of tick-borne encephalitis virus envelope proteins induced by an acidic pH. *J Virol*, 1995. 69(2): 695-700.

43. Kravats A., Jayasinghe M., Stan G. Unfolding and translocation pathway of substrate protein controlled by structure in repetitive allosteric cycles of the ClpY ATPase. *PNAS*, 2011. 108(6): 2234-2239.

44. Rogers D.M., Rempe S.B., Kent M.S. Calculation of the protein dissociation rate during membrane-protein centrifugation. *Unpublished work.*

45. Norde W., Haynes C. Reversibility and the mechanism of protein adsorption. 1995. In: Proteins at interfaces II. 1995. ACS Symposium Series. 602: 26-40.

46. Modis Y., Ogata S., Clements D., Harrison S.C. A ligand-binding pocket in the dengue virus envelope glycoprotein. *PNAS*, 2003. 100(12): 6986-6991.

47. Heinz F.X., Kunz C. Chemical crosslinking of tick-borne encephalitis virus and its subunits. *J Gen Virol*, 1980. 46: 301-309.

48. Chatterjee P.K., Vashishtha M., Kielian M. Biochemical consequences of a mutation that controls the cholesterol dependence of semliki forest virus fusion. *J Virol*, 2000. 74(4): 1623-1631.

49. Nanda H., Datta S.A.K., Heinrich F., Lösche M., Rein A., Krueger S., Curtis J.E. Electrostatic interactions and binding orientation of HIV-1 matrix studies by neutron reflectivity. *Biophys J*, 2010. 99: 2516-2524.

50. Benkoski J.J., Jesorka A., Edvardsson M., Höök F. Light-regulated release of liposomes from phospholipid membranes *via* photoresponsive polymer-DNA conjugates. *Soft Matter*, 2006. 2: 710-715.

51. Shenoy S., Shekhar P., Heinrich F., Daou M-C., Gericke A., Ross A.H., Lösche M. Membrane association of the PTEN tumor suppressor: molecular details of the protein-membrane complex from SPR binding studies and neutron reflection. *PLoS ONE*, 2012. 7(4): 1-13.

52. Ramsden J.J. Experimental methods for investigating protein adsorption kinetics at surfaces. *Quar Rev Biophys*, 1993. 27(1): 41-105.

53. Andre G., Brasseur R., Dufrêne Y.F. Probing the interaction forces between hydrophobic peptides and supported lipid bilayers using AFM. *J Mol Recongit*, 2007. 20: 538-545.

54. Ganchev D.N., Rijkers D.T.S., Snel M.M.E., Killian A., Kruijff B. Strength of Integration of Transmembrane α-helical peptides in lipid bilayers as determined by atomic force microscopy. *Biochem*, 2004. 43: 14987-14993.

55. Sieben C., Kappel C., Zhu R., Wozniak A., Rankl C., Hinterdorfer P., Grubmüller H., Herrmann A. Influenza virus binds to its host cell using multiple dynamic interactions. *PNAS*, 2012. 109(34): 13626-13631.

56. Cohen F.S., Melikyan G.B. The energetics of membrane fusion from binding, through hemifusion, pore formation, and pore enlargement. *J Membrane Biol*, 2004. 199: 1-14.

57. Evans E. Introductory lecture: energy landscapes of biomolecular adhesion and receptor anchoring at interfaces explored with dynamic force spectroscopy. *Faraday Discuss*, 1998. 111: 1-16.

58. Gerlach H., Laumann V., Martens S., Becker C.F., Goody R.S., Geyer M. HIV-1 Nef membrane association depends on charge, curvature, composition, and sequence. *Nat Chem Biol*, 2010. 6(1): 46-53.

59. Schmidt A.G., Lee K., Yang P.L., Harrison S.C. Small-molecule inhibitors of dengue-virus entry. *PLoS Path*, 2012. 8(4): 1-10.